cmgh
CELLULAR AND MOLECULAR GASTROENTEROLOGY AND HEPATOLOGY

ORIGINAL RESEARCH

Requirement of $G\alpha_q/G\alpha_{11}$ Signaling in the Preservation of Mouse Intestinal Epithelial Homeostasis

Noboru Watanabe,[1] Hirosato Mashima,[1,2] Kouichi Miura,[1] Takashi Goto,[1] Makoto Yoshida,[3] Akiteru Goto,[3] and Hirohide Ohnishi[1]

[1]Department of Gastroenterology and Hepato-Biliary-Pancreatology, [3]Department of Pathology, Akita University Graduate School of Medicine, Akita, Japan; [2]Department of Gastroenterology, Saitama Medical Center, Jichi Medical University, Saitama, Japan

SUMMARY

Gut hormones are important in coordinated actions of intestine and they exert actions through G-protein–coupled receptors. We show that $G\alpha_{q/11}$-mediated signaling plays a pivotal role in the maturation and positioning of Paneth cells and in the maintenance of intestinal homeostasis.

BACKGROUND & AIMS: Proliferation, differentiation, and morphogenesis of the intestinal epithelium are tightly regulated by a number of molecular pathways. Coordinated action of intestine is achieved by gastrointestinal hormones, most of which exert these actions through G-protein–coupled receptors. We herein investigated the role of $G\alpha_{q/11}$-mediated signaling in intestinal homeostasis.

METHODS: Intestinal tissues from control (*Gnaq*$^{flox/flox}$ *Gna11*$^{+/+}$), Int-G_q knock-out (KO) (*VilCre*$^{+/-}$*Gnaq*$^{flox/flox}$ *Gna11*$^{+/+}$), G_{11} KO (*Gnaq*$^{flox/flox}$*Gna11*$^{-/-}$), and Int-G_q/G_{11} double knock-out (DKO) (*VilCre*$^{+/-}$*Gnaq*$^{flox/flox}$*Gna11*$^{-/-}$) mice were examined by microscopy, transmission electron microscopy, and immunohistochemistry. The effect of $G\alpha_{q/11}$-mediated signaling was studied in the cell lineage, proliferation, and apoptosis. Dextran sodium sulfate (DSS) colitis was induced to study the role of $G\alpha_{q/11}$ in colon.

RESULTS: Paneth cells were enlarged, increased in number, and mislocalized in Int-Gq/G11 DKO small intestine. Paneth cells also reacted with PAS and Muc2 antibody, indicating an intermediate character of Paneth and goblet cells. The nuclear β-catenin, T-cell factor 1, and Sox9 expression were reduced severely in the crypt base of Int-Gq/G11 DKO intestine. Proliferation was activated in the crypt base and apoptosis was enhanced along the crypt. Int-Gq/G11 DKO mice were susceptible to DSS colitis. Proliferation was inhibited in the crypt of unaffected and regenerative areas. Cystic crypts, periodic acid–Schiff–positive cells, and Muc2-positive cells were unusually observed in the ulcerative region.

CONCLUSIONS: The $G\alpha_{q/11}$-mediated pathway plays a pivotal role in the preservation of intestinal homeostasis, especially in Paneth cell maturation and positioning. Wnt/β-catenin signaling was reduced significantly in the crypt base in $G\alpha_q/G_{11}$-deficient mice, resulting in the defective maturation of Paneth cells, induction of differentiation toward goblet cells, and susceptibility to DSS colitis. *(Cell Mol Gastroenterol Hepatol 2016;2:767–782; http://dx.doi.org/10.1016/j.jcmgh.2016.08.001)*

Keywords: Paneth Cell; Intermediate Cell; Wnt; *Gnaq*; *Gna11*.

The epithelium of small intestine is composed of 4 distinct cell lineages: absorptive enterocytes and 3 secreting cell types including mucus-secreting goblet cells, antimicrobial peptide-secreting Paneth cells, and hormone-secreting enteroendocrine cells. All of these cell types originate from multipotent stem cells residing in niches in the lower parts of the crypt. Cell renewal, lineage commitment, and cell differentiation in the intestinal epithelium are coupled to cell migration in a precise, spatially organized manner.[1] Stem cells give rise to progenitor cells, which are amplified by constant division along the bottom two thirds of the crypts.[2] These daughter cells migrate up as they proliferate. In the transit-amplifying zone near the top of the crypt, these cells terminally differentiate into the 4 main cell types. Then, absorptive enterocytes, goblet cells, and enteroendocrine cells migrate up the villi and Paneth cells migrate down to reside at the crypt base. The epithelium of large intestine lacks Paneth cells.

The digestive tract consists of a variety of tissues, each with a specific function necessary for the effective handling of a meal. The coordination of the complex functions of digestion, absorption, and excretion of a meal is achieved largely by molecules of neuroendocrine origin.[3] Gastrointestinal hormones, including cholecystokinin, gastrin, secretin, histamine, glucose-dependent insulinotropic polypeptide, glucagon-like-peptide-1, and vasoactive intestinal peptide, regulate their target cells through guanine

Abbreviations used in this paper: **Atoh1, atonal homolog 1; BrdU, bromodeoxyuridine; Defa1, defensin α1; Dll1, delta-like 1; DSS, dextran sodium sulfate; FGF, fibroblast growth factor; Fzd, frizzled; Hes, hairy/enhancer of split; IEC, intestinal epithelial cell; Ihh, Indian hedgehog; mRNA, messenger RNA; NICD, Notch intracellular cytoplasmic domain; PAS, periodic acid–Schiff; PCR, polymerase chain reaction; PKC, protein kinase C; qPCR, quantitative real-time polymerase chain reaction; Tcf, T-cell factor; TEM, transmission electron micrograph; TUNEL, terminal deoxynucleotidyl transferase-mediated deoxyuridine triphosphate nick-end labeling.**

Most current article

2352-345X
http://dx.doi.org/10.1016/j.jcmgh.2016.08.001

nucleotide-binding protein-coupled receptors (G-protein–coupled receptors). Another important group of modulators are neurotransmitters, such as acetylcholine, which are released from vagal nerve terminals and exert their roles through the muscarinic receptor subtype M3. Secretin, glucose-dependent insulinotropic polypeptide, and glucagon-like-peptide-1 exert their signals through the $G\alpha_s$ family of heterotrimeric G proteins.[4] In contrast, cholecystokinin, gastrin, and acetylcholine exert their signals through the $G\alpha_q$ family of G proteins. Mammals express 4 $G\alpha_q$ class α-subunits, of which 2, $G\alpha_q$ and $G\alpha_{11}$, are widely expressed[5]; their activation results in the stimulation of phospholipase C-β isoform and consequent inositol 1,4,5-triphosphate-mediated intracellular calcium mobilization and protein kinase C (PKC) activation.[6] The expression of $G\alpha_{14}$ and $G\alpha_{15/16}$ is restricted to certain tissues, such as kidney and hematopoietic organs, respectively.[7,8]

The gastrointestinal system is a rich source of neuroendocrine hormones that interact with at least 10 families of G-protein coupled receptors containing more than 30 known receptor subtypes.[3] Although the physiological relevance in the regulation of intestinal homeostasis remains unclear, the sheer number of potential $G\alpha_{q/11}$-coupled receptors suggests an importance of this G-protein family in the intestine.

Proliferation, differentiation, and morphogenesis in the intestinal epithelium are tightly regulated by a number of molecular pathways. Stem cells generate daughter cells that undergo lineage commitment and maturation through the combined action of the Wnt/β-catenin and Notch signaling pathways. Cells adopt either an absorptive or a secretory cell fate according to the balance between Wnt and Notch signaling.[9] Both pathways also regulate transcription networks that further define the differentiation of intestinal epithelial cells (IECs).[10]

The most established effects of Wnt/β-catenin in IECs are those involved in cell proliferation, in particular by maintaining the proliferative state of progenitors.[11] However, Wnt/β-catenin signaling is not confined to proliferating immature cells, but also is active in fully differentiated Paneth cells.[11] Wnt/β-catenin signaling maintains the correct positioning of the Paneth cells by controlling the expression of genes encoding ephrin B2/B3 receptors and the ephrin B1 ligand[1] and terminal maturation of Paneth cells.[11–15]

The Notch cascade mediates cell-to-cell signaling and has been shown to be essential for the maintenance of the proliferative crypt compartment, as well as for the formation of absorptive enterocytes.[10] Notch signaling occurs when the transmembrane Notch receptor is bound by ligands expressed on adjacent cells. The intracellular cytoplasmic domain of the receptor is cleaved from the transmembrane domain by γ-secretase and translocates to the nucleus, where it associates with the transcriptional activator protein RBP-Jk (CSL/CBF/Su[H]/Lag-1) to stimulate the expression of target genes, such as Hairy/enhancer of split 1 (Hes1) and Hes5.[16] Progenitor cells that express Hes1 will differentiate into absorptive enterocytes, whereas progenitors that express atonal homolog 1 (Atoh1, also known as Math1) are committed to the secretory lineage, differentiating into goblet, Paneth, or enteroendocrine cells. Goblet and Paneth cells continue to share similar characteristics, whereas the differentiation of secretory precursors into endocrine fate is regulated by neurogenin3.[17]

To study the role of the $G\alpha_q$ class of G proteins in intestinal homeostasis, we generated and examined mice with intestine-specific knockout of the genes encoding $G\alpha_q$ and $G\alpha_{11}$. We herein show that the $G\alpha_{q/11}$-mediated signaling pathway plays a pivotal role in Paneth cell maturation and positioning. It also plays a critical role in the maintenance of intestinal homeostasis.

Materials and Methods

Animals

C57BL/6 (B6) $Gnaq^{flox/flox}Gna11^{-/-}$ mice were kindly provided by Dr Stefan Offermanns of the Institute of Pharmacology, University of Heidelberg (Germany). To delete *Gnaq* in intestinal epithelial cells in adult mice, we crossed $Gnaq^{flox/flox}Gna11^{-/-}$ mice to Villin-Cre transgenic mice, which express Cre recombinase under the control of the villin promoter.[18] The villin promoter drives stable and homogeneous expression of Cre recombinase in nearly all epithelial cells in the small intestine and, to a lesser extent, the large intestine.[18]

All mice were maintained in a specific pathogen-free animal facility with free access to food and water, except for during experiments on dextran sodium sulfate (DSS)-induced colitis. All experiments using mice were approved by the Institutional Animal Care and Use Committee of Akita University.

Polymerase Chain Reaction for Genotyping, Conventional Reverse-Transcription Polymerase Chain Reaction, and Quantitative Real-Time Polymerase Chain Reaction

The primers used in this study are listed in Supplementary Table 1. Genomic DNA was isolated from mouse tails and amplified by standard polymerase chain reaction (PCR). Total RNA was obtained from IECs using an RNeasy Mini kit (Qiagen, Valencia, CA), which were scraped off the intestinal tissue with a spatula. First-stranded complementary DNA was synthesized from total RNA using Superscript First-stranded Synthesis System for reverse-transcription PCR (Invitrogen, Carlsbad, CA) according to the manufacturer's instructions. Quantitative real-time PCR (qPCR) was performed using ABI PRISM 7900HT (Applied Biosystems, Foster City, CA): denaturation at 94°C for 30 seconds, annealing at 60°C for 30 seconds, and extension at 72°C for 30 seconds.

Materials

The primary antibodies used in the studies are listed in Supplementary Table 2. Horseradish-peroxidase–conjugated donkey anti-mouse IgG, horseradish-peroxidase–conjugated donkey anti-rabbit IgG, horseradish-peroxidase–conjugated donkey anti-goat IgG, and Cy3-conjugated donkey anti-rabbit IgG were from Jackson Immuno Research (West Grove, PA). DSS (molecular weight, 36–50 kilodaltons) was purchased from MP Biomedicals (Solon, OH).

Immunohistochemistry

Eight- to 10-week-old mice were killed, and the intestinal tissues were excised. Formalin-fixed and paraffin-embedded samples or frozen sections were used for immunohistochemistry. Detection of β-catenin staining was performed using the Envision+ system (Dako, Glostrup, Denmark). Tyramide signal amplification (Molecular Probes, Waltham, MA) was used for the immunofluorescent detection of delta-like 1 (Dll1). Staining was visualized by secondary antibodies or tyramide substrates conjugated with Alexa-594 (Molecular Probes). Nuclei were counterstained with hematoxylin (Wako Chemicals, Doshoumachi, Osaka) or with 4′,6-diamidino-2-phenylindole (Invitrogen, Carlsbad, CA). Light microscopy and immunofluorescence microscopy were performed as described previously.[19] For the electron microscopy, small tissue pieces from intestine were post-fixed with 2.5% glutaraldehyde and 1% OsO_4 and embedded in an epoxy resin. Semithin and ultrathin sections were stained with toluidine blue and uranyl acetate/lead citrate for observation under both a light microscope and an electron microscope, respectively. The ultrastructural analysis and quantification of intestinal crypts and villi were determined on random micrographs showing the full face of the structure, where the crypt and villi clearly were identified. Quantitative analyses were measured using ImageJ software (National Institutes of Health, Bethesda, MD).

Western Blotting

IECs, which had been scraped from intestinal tissue using a spatula, were homogenized in a lysis buffer (100 mmol/L NaCl, 20 mmol/L Tris/HCl, pH 7.5, and 1% Triton X-100; Sigma-Aldrich, St. Louis, MO). After centrifugation, the crude extracts were boiled in Laemmli 2× sample buffer. Twenty to 50 μg of protein was loaded onto each lane of 5%–15% sodium dodecyl sulfate-polyacrylamide gels and run at 200 V. The proteins then were transferred onto nitrocellulose membranes at 60 V for 4 hours. The membranes were incubated sequentially with Blocking Ace (Snow Brand Milk Products, Sapporo, Japan), primary antibodies and secondary antibodies, and then were detected using an enhanced chemiluminescence Western blot detection reagent (Amersham Biosciences, Piscataway, NJ) to visualize the secondary antibody. The densitometry analysis was performed using the ImageJ software program.

Terminal Deoxynucleotidyl Transferase-Mediated Deoxyuridine Triphosphate Nick-End Labeling Assay

Apoptotic cells were detected using an In Situ Cell Death Detection Kit, TMR red (Roche Applied Science, Mannheim, Germany) according to the manufacturer's instructions. The nuclei were counterstained with 4',6-diamidino-2-phenylindole. The number of terminal deoxynucleotidyl transferase-mediated deoxyuridine triphosphate nick-end labeling (TUNEL)-positive cells was counted at a magnification of ×200 with an Olympus IX70 fluorescence microscope (Shinjuku, Tokyo).

Induction of DSS Colitis and Grading of Histologic Changes

DSS (molecular weight, 36–50 kilodaltons) was added to the drinking water of the mice at a final concentration of 3% (wt/vol) for 5 consecutive days (days 1–5), followed by distilled water.[20] The whole body weights of mice were measured every day. Some of the mice were killed at the indicated times and colonic samples were subjected to H&E staining, histology, and immunohistochemistry.

Statistical Analysis

All data are presented as the means ± SD. The Student *t* test was used to compare the values between 2 mice lines and a 1-way analysis of variance, and post hoc tests were used for comparisons among the 4 mouse lines. *P* values less than .05 were considered to indicate statistical significance.

Results

The Generation of Intestinal Epithelial Cell–Specific $G\alpha_q/G\alpha_{11}$-Deficient Mice

To generate intestinal epithelial cell–specific $G\alpha_q/G\alpha_{11}$-deficient mice, we crossed the *VilCre* mouse line[18] with mice carrying floxed alleles of the gene coding for $G\alpha_q$, *Gnaq* (*Gnaq*$^{flox/flox}$),[21] and constitutive $G\alpha_{11}$-deficiency (*Gna11*$^{-/-}$).[22] In the *VilCre* mouse line, Cre recombinase is expressed specifically in the intestinal epithelium from 10.5 days postcoitum onward.[18] We generated 4 mouse lines: control mice (*Gnaq*$^{flox/flox}$*Gna11*$^{+/+}$, henceforth termed control), intestine-specific $G\alpha_q$-deficient mice (*VilCre*$^{+/-}$*Gnaq*$^{flox/flox}$*Gna11*$^{+/+}$, termed Int-G_q knock-out), $G\alpha_{11}$-deficient mice (*Gnaq*$^{flox/flox}$*Gna11*$^{-/-}$, termed G_{11} KO), and intestine-specific $G\alpha_q/G\alpha_{11}$-double-deficienct mice (*VilCre*$^{+/-}$*Gnaq*$^{flox/flox}$*Gna11*$^{-/-}$, termed Int-G_q/G_{11} double knock-out). These mice were born at the expected numbers, were fertile, and showed no obvious abnormalities. Their body weights did not differ from that of C57BL/6 wild-type mice or *VilCre* mice (*VilCre*$^{+/-}$*Gnaq*$^{+/+}$*Gna11*$^{+/+}$) (data not shown). PCR analysis and Western blot of intestinal mucosa showed a clear reduction in the expressions of $G\alpha_q$ and $G\alpha_{11}$ in these mouse lines, particularly in Int-G_q/G_{11} DKO mice (Figure 1*A* and *B*). The band intensity of *Gna11* in PCR analysis and $G\alpha_{11}$ on Western blot was stronger than that of *Gnaq* and $G\alpha_q$. This may be owing to the abundant expression of $G\alpha_{11}$ in mouse small intestine compared with $G\alpha_q$.[5] In contrast, on Western blot of large intestine, the band intensity of $G\alpha_q/G\alpha_{11}$ in Int-G_q KO and G_{11} KO mice was reduced to almost the same level. This may imply that $G\alpha_q$ and $G\alpha_{11}$ were expressed in nearly equal quantities in the large intestine (Supplementary Figure 1*A*). Immunoreactivity for $G\alpha_q/G\alpha_{11}$ was observed primarily in the basolateral membrane of the cells in the villi and crypts and in the cells in the lamia propria. It clearly disappeared in the IECs of Int-G_q/G_{11} DKO mice, but not in the cells in lamia propria (Figure 1*C*). The loss of $G\alpha_q/G\alpha_{11}$ in the intestinal mucosa resulted in a significant reduction in the PKC phosphorylation of several isoforms, whereas the

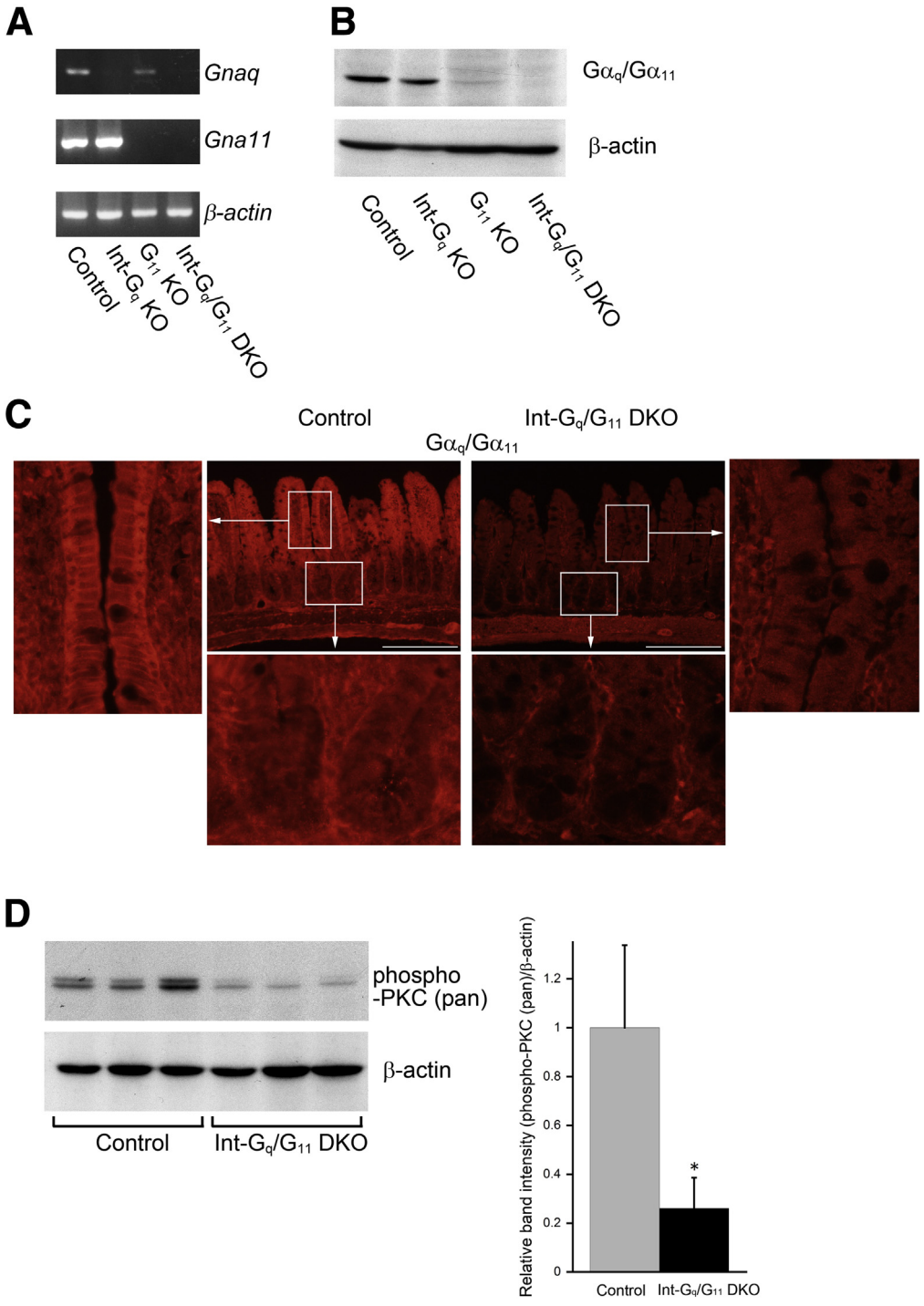

Figure 1. The expression of $G\alpha_q$ and $G\alpha_{11}$ in small intestinal epithelial cells in 4 mouse lines: control (*Gnaq*$^{flox/flox}$*Gna11*$^{+/+}$), Int-G_q KO (*VilCre*$^{+/-}$ *Gnaq*$^{flox/flox}$*Gna11*$^{+/+}$), G_{11} KO (*Gnaq*$^{flox/flox}$*Gna11*$^{-/-}$), and Int-G_q/G_{11} DKO (*VilCre*$^{+/-}$*Gnaq*$^{flox/flox}$*Gna11*$^{-/-}$). (*A*) Reverse-transcription PCR analysis of mRNA expression for *Gnaq* and *Gna11* in small intestine. (*B*) Western blot analysis of $G\alpha_q$/$G\alpha_{11}$ expression. (*C*) Immunohistochemical detection of $G\alpha_q$/$G\alpha_{11}$ expression in small intestine of control and Int-G_q/G_{11} DKO mice. *Lower* and *side panels* show the *boxed areas* with higher magnification. *Scale bars*: 200 μm. (*D*) Western blot analysis of the phosphorylation of PKC. This antibody detects endogenous levels of PKC α, βI, βII, δ, ε, η and θ isoforms when it is phosphorylated at a carboxyl terminal residue homologous to serine 660 of PKC βII. *Right*: ImageJ densitometry analysis. The values represent the means ± SD (n = 3). *P < .05.

messenger RNA (mRNA) levels of PKCα and PKCδ were not changed (Figure 1*D* and Supplementary Figure 2).

Paneth Cells Are Enlarged, Increased in Number, and Mislocalized in Int-G_q/G_{11} DKO Intestine

To investigate whether intestine-specific inactivation of $G\alpha_q$/$G\alpha_{11}$ affected the homeostasis of IECs, we performed histologic and immunohistochemical studies. The general morphology and architecture of the intestinal tract from 2- to 6-month-old adult mice were unaffected. However, H&E staining showed that $G\alpha_q$/$G\alpha_{11}$ deficiency led to the enlargement of Paneth cells with characteristic eosinophilic staining in Int-G_q/G_{11} DKO intestine (Figure 2*A*). Moreover, such cells were observed in the upper part of crypt and villi (Figure 2*A* and

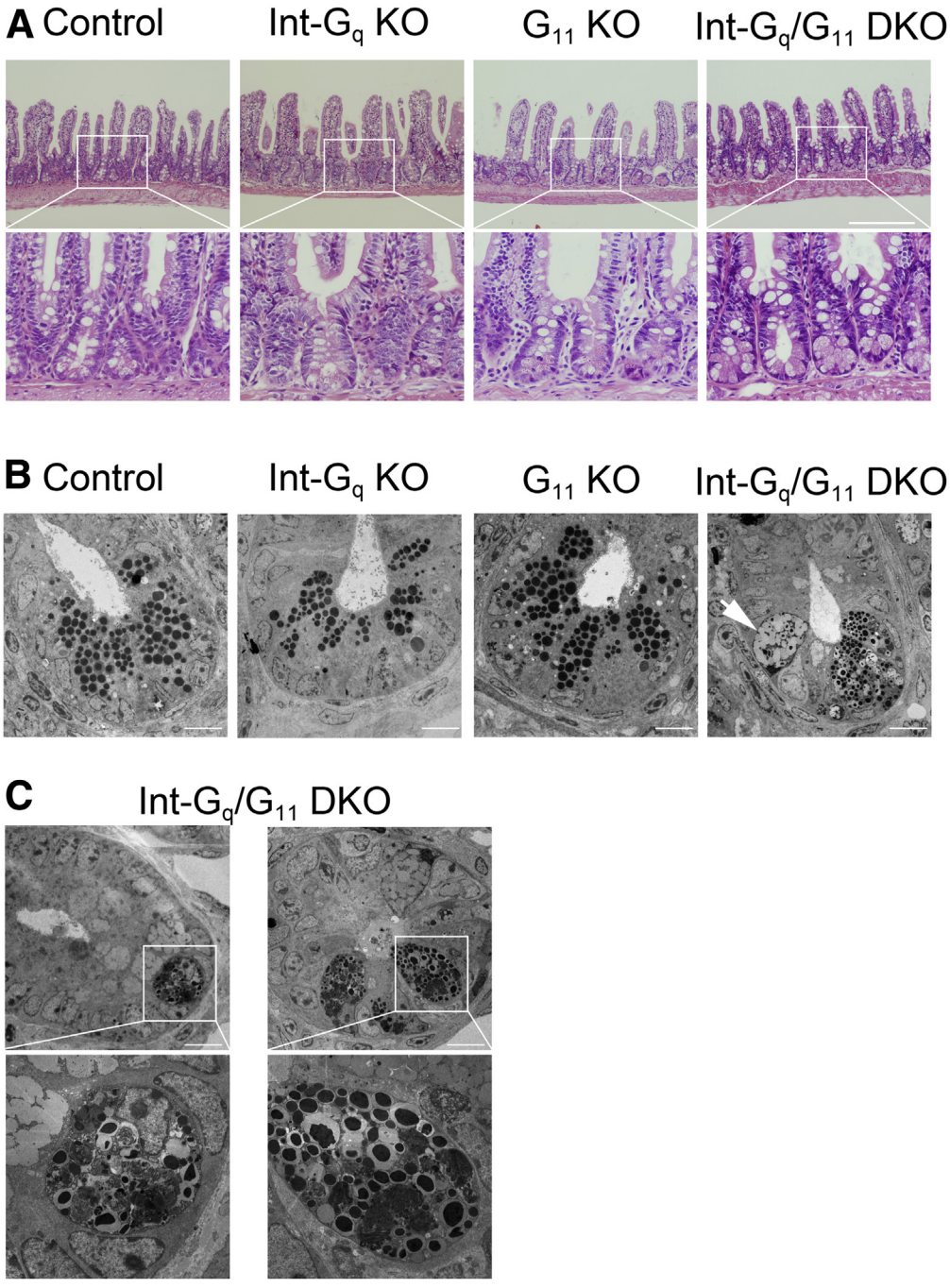

Figure 2. Morphologic studies of small intestine in 4 mouse lines. (*A*) H&E staining in small intestine. *Scale bar*: 200 μm. The enlargement of Paneth cells with characteristic eosinophilic staining was observed in the crypt of Int-G_q/G_{11} DKO mice. Slightly enlarged Paneth cells also were observed in G_{11} KO mice. In contrast, the alteration was not observed in Int-G_q KO mice. (*B*) Transmission electron micrographs in the crypt. *Scale bars*: 10 μm. Paneth cells in G_q/G_{11}-deficient crypts showed a bipartite structure in their secretory granules: a smaller electron-dense core and a peripheral halo. An unusually large granulomucous cell also was observed (*arrow*). (*C*) Unhealthy-looking Paneth cells in G_q/G_{11}-deficient crypts. *Scale bars*: 10 μm. Electron-dense materials might be degraded in a cell.

Supplementary Figure 1*B*, arrowheads). G_{11} KO Paneth cells showed a similar, but slight, alteration. In contrast, Paneth cells were localized to the crypt base and the alteration was not observed in Int-G_q KO mice (Figure 2*A*). No apparent macroscopic or microscopic phenotype was observed in large intestine in these 4 mouse lines (Supplementary Figure 1*C*).

We next examined the transmission electron micrographs (TEM) of these mice. In Paneth cells of Int-G_q/G_{11} DKO mice, secretory granules showed a bipartite structure with a small, round central core of high electron density and a peripheral halo of lower density. The diameter of high electron density was much smaller than that in the other 3 types of mice. This feature resembles intermediate cells (intermediate between goblet cells and Paneth cells), which are considered to be rare cells in the transition between undifferentiated cells and more mature secretory cells.[23] An unusually large granulomucous cell also was observed (Figure 2*B*, arrow). In addition, unhealthy-looking cells were observed in Int-Gαq/Gα11 DKO crypts. Electron-dense granules and intracellular materials appeared to be degraded in these cells (Figure 2*C*).

Next, we investigated whether Int-G_q/G_{11} DKO IECs showed correct differentiation along the 4 intestinal epithelial cell lineages. H&E staining showed an enlargement of Paneth cells in Int-G_q/G_{11} DKO crypt, whereas the electron-dense area in secretory granules was much smaller in TEM. Then, immunohistochemistry for lysozyme, an early marker of Paneth cell specification, was examined (Figure 3*A*). Lysozyme staining confirmed that the enlarged cells at the crypt base of Int-G_q/G_{11} DKO intestine expressed a key Paneth cell biomarker and lysozyme-positive cells were distributed abnormally above the crypt base. In the G_{11} KO mice, the lysozyme-positive cells were slightly enlarged. We quantified the number of lysozyme-positive cells in the crypt and villi. As shown in Figure 3*B*, the number of lysozyme-positive cells was increased both in crypt and villi in the G_{11} KO and Int-G_q/G_{11} DKO intestine. The Paneth cells showed an aberrant morphology because lysozyme-positive cells were enlarged in size, increased in number, and mislocalized in the crypt and villi on $G\alpha_{q/11}$ deletion. The number of mispositioned Paneth cells was increased gradually toward the distal part of ileum (data not shown). This may coincide with the expression of Cre recombinase.[18] Subsequent studies were performed using the distal part of ileum.

Expansion of Intermediate Cells in Crypt and Villi in Int-Gq/G_{11} DKO Intestine

Next, we performed periodic acid–Schiff (PAS) staining, Alcian blue staining, and immunohistochemistry for Muc2 to examine the goblet cells (Figure 3*A* and Supplementary Figure 3). When compared with control, PAS reactivity clearly was increased in both the crypts and villi of G_{11} KO and Int-G_q/G_{11} DKO IECs (Figure 3*A*). For confirmation, we quantified the number of PAS-positive cells (Figure 3*C*). In the G_{11} KO and Int-G_q/G_{11} DKO small intestine, the number of PAS-positive cells was increased significantly in both the crypts and villi (Figure 3D). The number of PAS-positive cells also was increased in the villi of the Int-G_q KO small intestine. The size of PAS-positive cells was increased in Int-G_q/G_{11} DKO crypt (1.7-fold, in comparison with control). The quantification of Alcian blue–stained cells and Muc2-positive cells showed similar results (Supplementary Figure 3, data not shown).

The increase in the number of lysozyme-positive cells and PAS-positive cells within crypt on $G\alpha_{q/11}$ deficiency suggested that some of these cells were dual-positive, expressing both Paneth and goblet cell markers, which is referred to as intermediate cells in the literature.[23–25] We then performed simultaneous lysozyme and PAS staining. As expected, dual-positive cells were increased significantly in number in the G_{11} KO and Int-G_q/G_{11} DKO crypts (Figure 3*A* and *D*). In the villus region, all lysozyme-positive cells were PAS positive, the right panel in Figure 3*B* indicates the number of dual-positive cells in the villi.

We next evaluated enterocytes and enteroendocrine cells by staining for intestinal alkaline phosphatase, a differentiation marker of enterocytes, and chromogranin A, a commonly used marker for neuroendocrine cells. We also examined the cell polarity by staining for F-actin, mainly localized in the subapical area, and E-cadherin, a component of adherence junction. As shown in Figure 4, no significant differences were detected in these staining series between the control and Int-G_q/G_{11} DKO mice. There were no differences also in Int-G_q KO and G_{11} KO mice (data not shown). The number of chromogranin A–positive cells in crypt and villi showed similar results in the 4 genotypes.

These results indicate that the increase in lysozyme and PAS reactivity in $G\alpha_{q/11}$-deficient intestine was a result of an increased number of intermediate cells in crypt and villi and an increased number of goblet cells in villi. We observed a decrease in diameter of high electron density in Paneth cell granules with a peripheral halo in TEM of Int-G_q/G_{11} DKO crypt (Figure 2*B*), suggesting that the defective maturation of Paneth cells may be involved in the unusual features. Quantitative real-time PCR was performed using specific primers for Paneth cell markers, lysozyme and defensin α1 (Defa1). Although lysozyme mRNA level remained unchanged, the Defa1 mRNA level was decreased significantly in Int-G_q/G_{11} DKO mice (Supplementary Figure 2). This may be owing to the fact that Defa1 is a target gene of Wnt signaling whereas lysozyme is not.[16] The decrease in Defa1 mRNA level suggests that Paneth cells have not undergone full differentiation to the Paneth cell lineage in Int-G_q/G_{11} DKO mice.

$G\alpha_{q/11}$-Deficiency Reduces Wnt/β-Catenin Signaling in IECs, Especially in Paneth Cells

Paneth cell positioning in the normal adult intestinal epithelium is tightly regulated by canonical Wnt signaling and the consequent control over EphB3 expression.[1,27] Paneth cells located in the crypt base contain high levels of nuclear β-catenin.[1] Immunostaining with a β-catenin antibody showed membrane-localized β-catenin along the crypt–villus axis, as well as nuclear β-catenin in cells occupying basal positions of the crypt in control and Int-G_q KO mice (Figure 5*A*). In contrast, the lining enlarged cells at Int-G_q/G_{11} DKO crypt base were devoid of nuclear β-catenin staining; those in the G_{11} KO crypt base showed a decreased number of nuclear β-catenin–positive cells. Immunohistochemical staining for T-cell factor 1 (Tcf1; also known as transcription factor 7) showed similar results and a Western blot analysis showed the reduced expression of Tcf1 in the small intestinal mucosa of Int-G_q/G_{11} DKO mice (Figure 5*B* and *F*). The transcription factor Sox9 is a Wnt/β-catenin transcriptional target that is required for Paneth cell specification.[14,27] Sox9 was expressed in all epithelial cells in the lower two thirds of the crypts, namely in the domains of transiently proliferating cells and of Paneth cells in control and Int-G_q KO mice.[14,27] In Int-G_q/G_{11} DKO mice, nuclear staining of Sox9 disappeared in the enlarged cells at the crypt base and was reduced in number in G_{11} KO mice (Figure 5*C*). The Wnt receptor frizzled5 (Fzd5) plays a critical role in Wnt-dependent Paneth cell maturation and binds Wnt5a as a ligand.[15] There were no significant differences in the mRNA levels of Wnt5a, Fzd5, and Fzd7 in the control or Int-G_q/G_{11} DKO IECs, whereas the mRNA level of

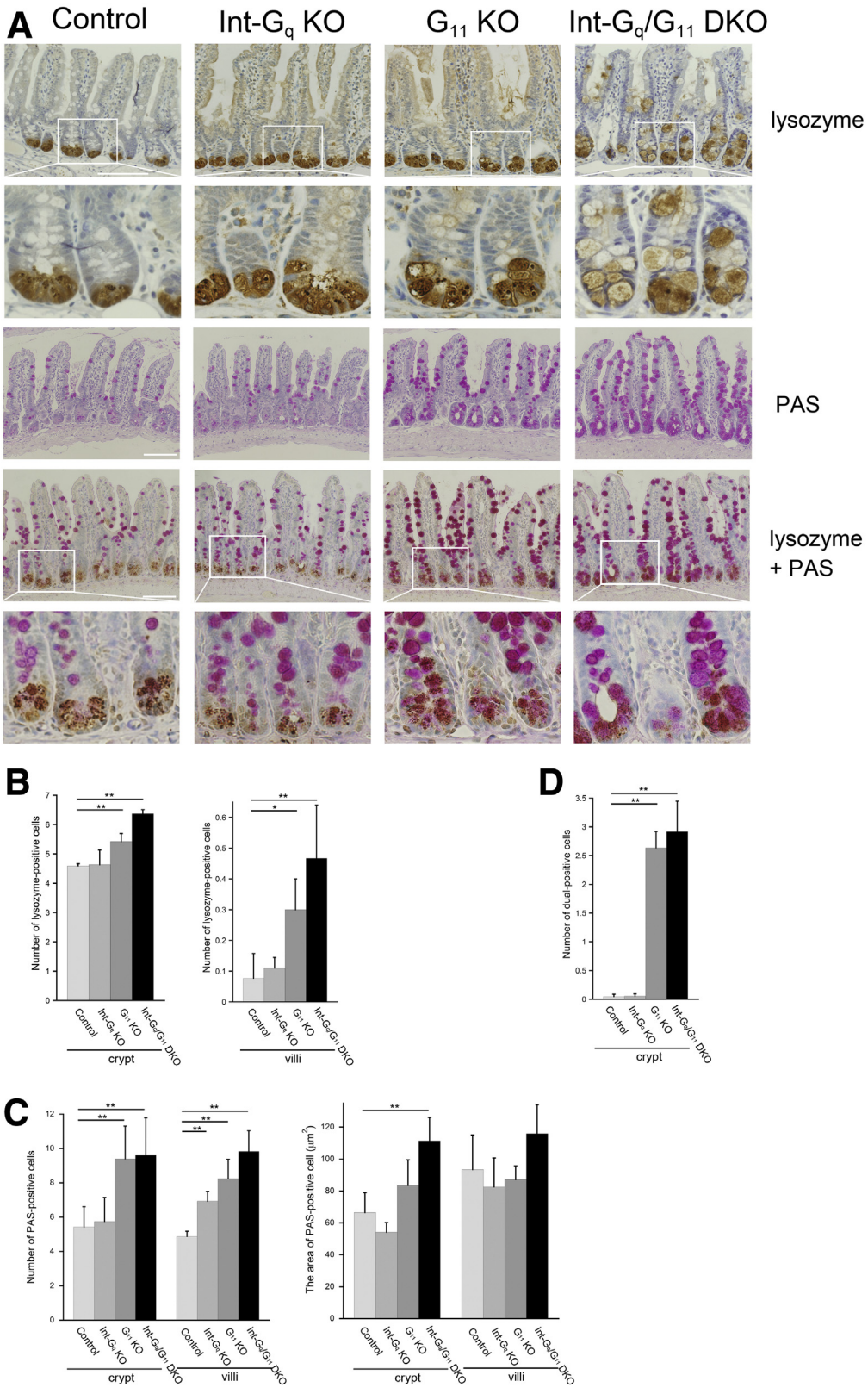

Figure 3. Disturbance of Paneth cells and goblet cells in $G\alpha_{q/11}$ deficiency. (*A*) Immunostaining showed that enlarged lysozyme-positive cells were mislocalized along crypt and villi in Int-G_q/G_{11} DKO intestine. G_{11} KO mice showed a similar but slight alteration. PAS staining indicated the expansion of mucin-containing cells both in the crypts and villi of G_{11} KO and Int-G_q/G_{11} DKO mice. Double-positive cells were observed in G_{11} KO and Int-G_q/G_{11} DKO crypts. *Scale bars*: 100 μm. (*B*) An analysis of the number of lysozyme-positive cells along crypt and villi. (*C*) An analysis of the number and area of PAS-stained cells along crypt and villi. (*D*) Quantification of dual-positive cells along the crypt. The cell number and size are graphed as the means ± SD (30 crypts and villi/mouse, n = 4 per genotype). Three independent experiments were performed with similar results. Representative figures are shown. $^*P < .05$, $^{**}P < .01$, according to an analysis of variance.

Tcf4 was reduced in Int-G_q/G_{11} DKO IECs (Supplementary Figure 2). A qPCR for canonical Wnt targets showed the decreased expression of Axin2, but not EphB3, EphB2, or Ascl2, in the Int-G_q/G_{11} DKO intestinal mucosa. These results suggest that $G\alpha_{q/11}$ deficiency reduces Wnt signaling partially in IECs, but strongly in Paneth cells.

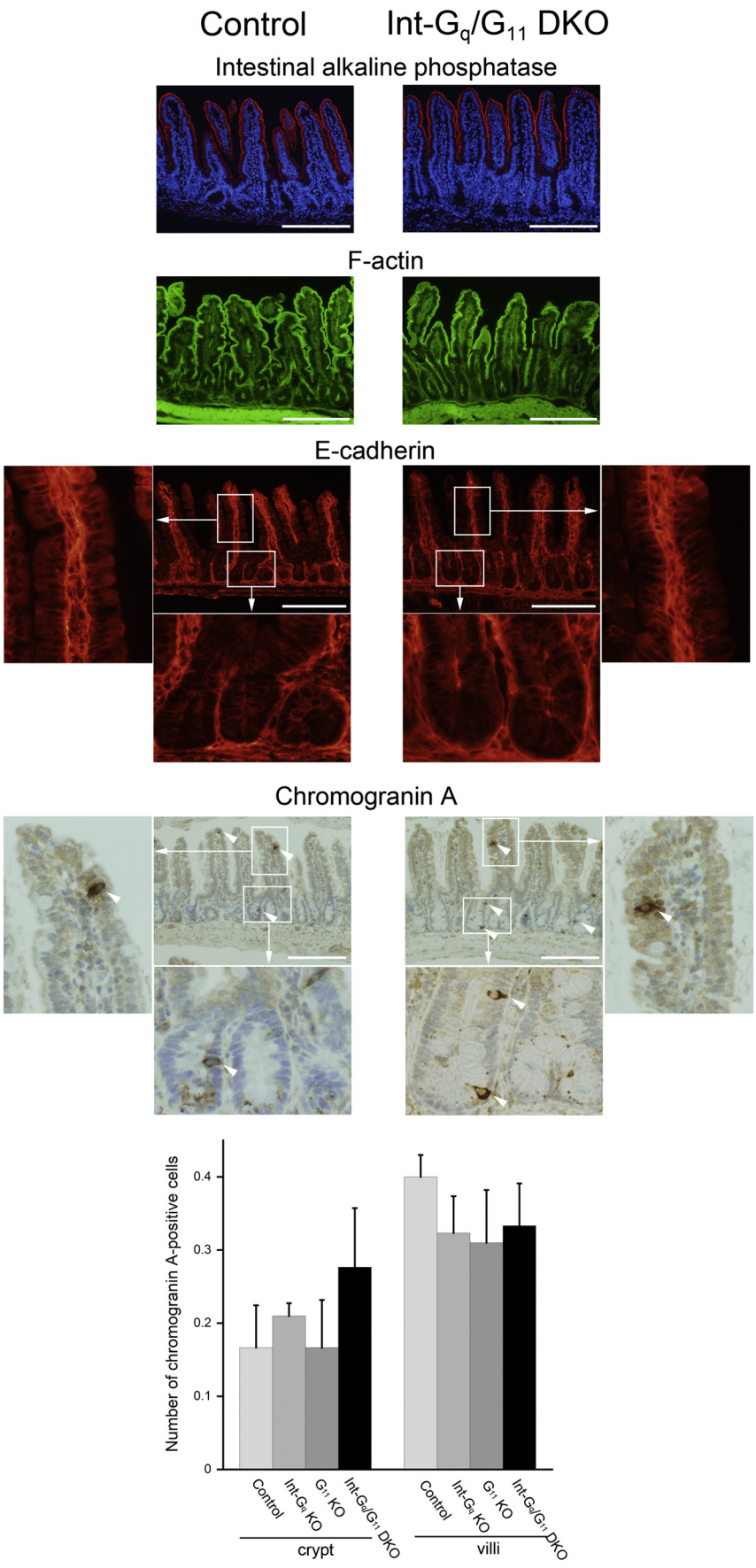

Figure 4. Preservation of enterocytes and enteroendocrine cells and cell polarity in $G\alpha_{q/11}$-deficient mice. Immunohistochemical studies were performed for intestinal alkaline phosphatase (enterocyte marker), chromogranin A (endocrine cell marker), F-actin (mainly localized in the subapical membrane), and E-cadherin (localized in the basolateral membrane). No differences were observed between control and Int-G_q/G_{11} DKO mice. *Scale bars*: 200 μm. *Bottom*: Analysis of the number of chromogranin A–positive cells (*arrowheads*) in crypt and villi in the 4 genotypes. Cell numbers are graphed as the means ± SD (30 crypts and villi/mouse, n = 4 per genotype).

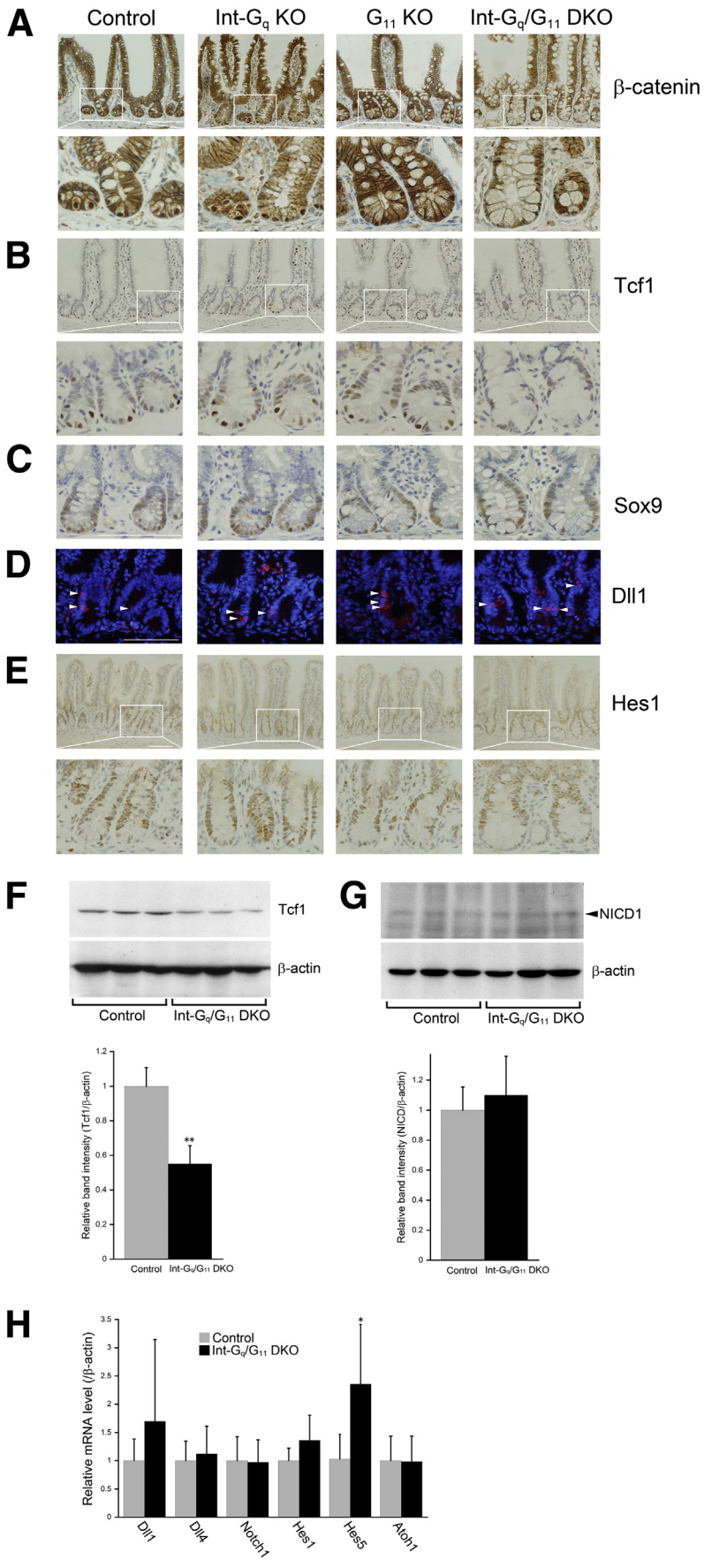

Figure 5. Reduction in Wnt/β-catenin signaling and a subtle alteration in Notch signaling in $G\alpha_{q/11}$-deficient IECs. Immunohistochemical studies were performed for (*A*) β-catenin, (*B*) Tcf1, (*C*) Sox9, (*D*) Dll1, and (*E*) Hes1. Immunoreactivities for nuclear β-catenin, Tcf1, and Sox9 were reduced in the crypt base of G_{11} KO and greatly in Int-G_q/G_{11} DKO mice compared with control and Int-G_q KO mice. *Scale bars*: 100 μm. Western blot was performed for the (*F*) Tcf1 and (*G*) NICD1. *Lower panel*: ImageJ densitometry analysis. (*H*) The relative mRNA expression in the Notch signaling molecules was evaluated by a quantitative real-time PCR. The data represent the means ± SD of 3 mice per genotype. Two independent experiments were performed with similar results (n = 3). $^{*}P < .05$, $^{**}P < .01$.

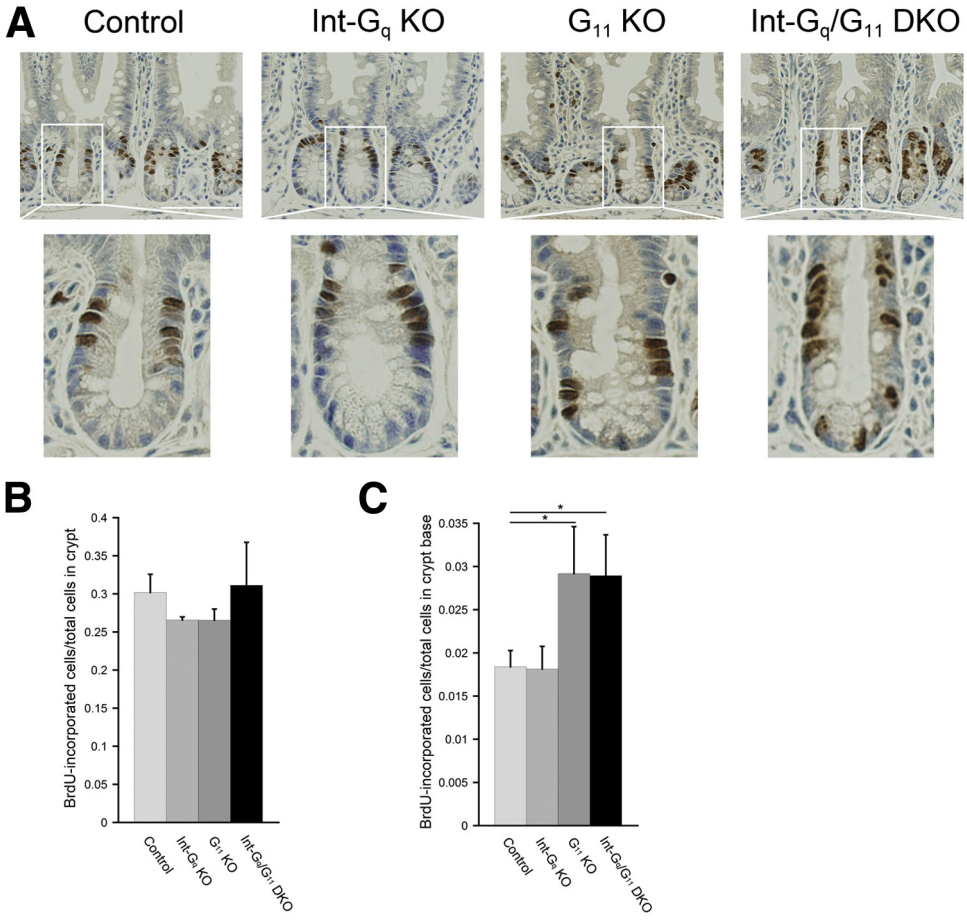

Figure 6. Increase of proliferation in crypt base and apoptosis in crypt of the $G\alpha_{q/11}$-deficient intestine. (*A*) Proliferation was examined by BrdU staining at 2 hours after the injection (*scale bars*: 100 microm). The number of BrdU-positive cells was counted in the (*B*) crypt and (*C*) crypt base (the lower third of the crypt). Cell numbers are graphed as the means ± SD (30 crypts/mouse; n = 3 per genotype). (*D*) Apoptotic cells were measured using a TUNEL assay (*arrowheads*; *scale bars*: 100 microm). (*E*) The number of TUNEL-positive cells was graphed as the means ± SD (30 crypts or villi/mouse; n = 3 per genotype). Three independent experiments were performed with similar results. Representative figures are shown. *$P < .05$.

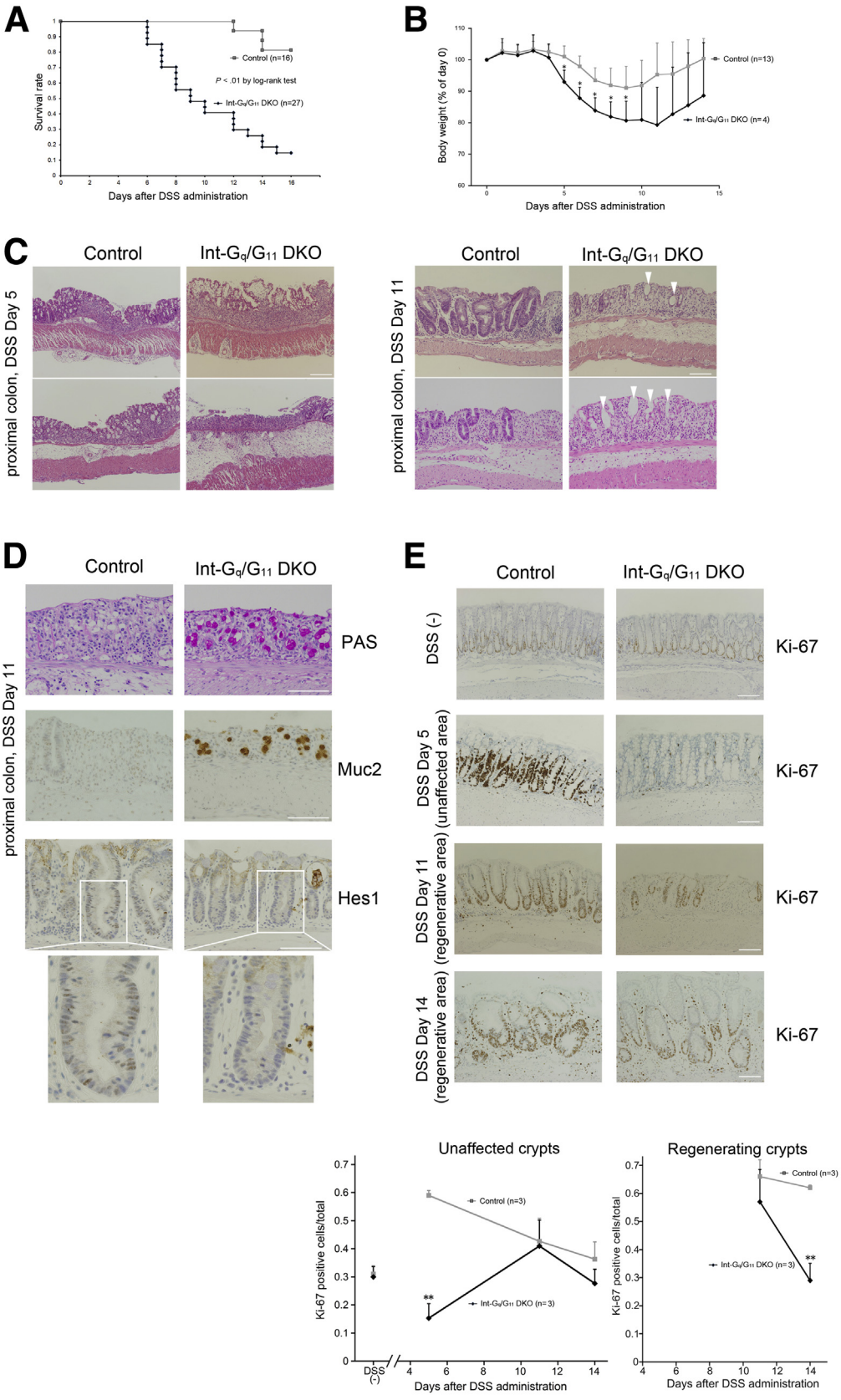

Figure 7. Requirement of $G\alpha_{q/11}$ signaling during regeneration of colonic epithelia in DSS colitis. (*A*) The survival rate was monitored until day 16 after the administration of DSS (n = 16 in control mice and n = 27 in Int-G_q/G_{11} DKO mice). (*B*) Body weight of the survivors (% of weight at day X/day 0) is graphed as the means ± SD (n = 13 in control mice and n = 4 in Int-G_q/G_{11} DKO mice). (*C*) H&E staining of a proximal colon specimen in the acute colitis stage (day 5 after the administration of DSS) and healing stage (day 11). Two representative images from independent mice are shown. Cystic crypts, lined with an epithelial layer that had lost the typical columnar cell appearance, were observed during the healing stage of Int-G_q/G_{11} DKO mice (*arrowheads*). (*D*) PAS-positive and Muc2-positive cells were observed in the ulcerative area of Int-G_q/G_{11} DKO proximal colon. Nuclear Hes1 immunoreactivity was decreased in the regenerating crypts of Int-G_q/G_{11} DKO colon. (*E*) Proliferation was examined in the proximal colon by immunohistochemistry for Ki-67. The rate of Ki-67–positive cells in the unaffected crypts (DSS (-), days 5, 11, and 14) and in the regenerating crypts (days 11 and 14) is graphed as the means ± SD (n = 3 per genotype). Three independent experiments were performed with similar results. Representative images and figures are shown. **P* < .05, ***P* < .01 (*scale bars*: 100 μm).

$G\alpha_{q/11}$ Deficiency Results in the Subtle Alteration in Notch Signaling

Notch signaling has been shown to play a pivotal role in secretory cell lineages.[16,28,29] Immunostaining of Dll1, one of the Notch signaling ligands, showed that there were no differences in the crypts of the 4 genotypes (Figure 5*D*). Immunostaining of Hes1, one of the important Notch signaling effectors, showed no significant changes (Figure 5*E*). A Western blot analysis to detect the Notch1 intracellular cytoplasmic domain (NICD1) showed no differences between control and Int-G_q/G_{11} DKO IECs (Figure 5*G*). A qPCR for Dll1, Dll4, Notch1, Hes1, and Atoh1 showed no changes, whereas Hes5 mRNA expression was increased in the Int-G_q/G_{11} DKO IECs (Figure 5*H*). This may coincide with the increased number of goblet cells in Int-G_q/G_{11} DKO IECs because Hes5 is expressed not only in the proliferating crypt, but also in the postmitotic cells in the lower villi,[30] and Hes5 activation has been reported to increase goblet cell numbers by driving the differentiation of postmitotic cells into mature goblet cells.[16]

Because Paneth cells are located next to putative stem cells, the defective maturation of Paneth cells may affect stem homeostasis. Activation of Wnt/β-catenin signaling pathway has been shown to be important not only for Paneth cell lineage allocation, but also for the regulation and maintenance of intestinal stem cells.[14,27] A number of transcription factors and kinases also are known to regulate cell fate specification of intestinal progenitors, including SAM pointed domain-containing Ets transcription factor (Spdef), Gfi1, and Stk11 (Lkb1).[31–33] We thus examined the expression levels of these genes and stem cell markers, leucine-rich repeat-containing G-protein-coupled receptor 5 and Bmi-1. Interestingly, the phenotype of mislocalized Paneth cells was indistinguishable from that of $LKB1^{-/-}$ mice.[33] However, we did not observe any significant changes in mRNA level, except that Cdx1 mRNA level was increased slightly but significantly in Int-G_q/G_{11} DKO intestine (Supplementary Figure 2).

Proliferation in the Crypt Base and Apoptosis Are Increased in $G\alpha_{q/11}$-Deficienct Mice

The increase in intermediate cell number may be related to the alteration of proliferation of IECs. To confirm this, a bromodeoxyuridine (BrdU) experiment was performed. Mice were injected with BrdU, euthanized 2 hours later, and the location and proportion of cells in the S phase were scored. Proliferative cells were restricted to the crypt compartment. The ratio of BrdU-labeled cells over the total number of cells along the crypt circumference was not altered in the 4 genotypes (Figure 6*A* and *B*). However, when we carefully counted BrdU-incorporated cells in the crypt base (the lower third of the crypt), there was a significant increase in G_{11} KO and Int-G_q/G_{11} DKO crypt (Figure 6*A* and *C*).

We next investigated apoptotic cells using a TUNEL assay. In control, Int-G_q KO, and G_{11} KO mice, apoptotic cells were found in the crypt only occasionally, however, more apoptotic cells were observed in the Int-G_q/G_{11} DKO crypt (Figure 6*D* and *E*, arrowheads).

Int-G_q/G_{11} DKO Mice Are Susceptible to DSS-Induced Colitis

There were no abnormalities found in the physiological condition of the $G\alpha_{q/11}$-deficient colonic epithelium (Supplementary Figure 1). Intermediate cells that we found in the $G\alpha_{q/11}$-deficient small intestine were reported to be observed during intestinal infection and inflammation.[34,35] We then induced acute colitis in control and Int-G_q/G_{11} DKO mice by the continuous administration of DSS (3%) in the drinking water for 5 days. DSS administration gradually induced symptoms resembling ulcerative colitis. Most of the mice developed bloody diarrhea and rectal bleeding 4 days after the administration of DSS, and these symptoms gradually worsened. Int-G_q/G_{11} DKO mice showed severe mortality after the administration of DSS (Figure 7*A*). Int-G_q/G_{11} DKO mice that survived showed a severe weight loss compared with control (Figure 7*B*). We then compared the histologic changes in the acute colitis stage (day 5 after the start of DSS administration) and healing stage (day 11). Histologic analyses on day 5 showed larger areas of ulceration, crypt loss, thickening of the mucosa with abundant edema, and more massive inflammatory cell infiltration into the mucosa and submucosa in the Int-G_q/G_{11} DKO proximal colon (Figure 7*C*). In the healing stage, we observed regenerating crypts in the injured area of control mice. In Int-G_q/G_{11} DKO mice, regeneration was reduced and instead cystic crypts, lined with an epithelial layer that had lost the typical columnar cell appearance, were observed in the ulcerative area (Figure 7*C*, arrowheads). Such structures rarely were observed in the ulcerative region of the control mice. When we measured and added the length of the ulcerative region where the cystic crypts were observed, the region was found to be significantly longer in Int-G_q/G_{11} DKO mice (control, 0.019 ± 0.038 mm/mouse; Int-G_q/G_{11} DKO, 6.4 ± 3.6 mm/mouse; n = 4 per genotype; $P = .04$). The total length of colon did not change between the 2 genotypes (data not shown). We next performed PAS staining and immunohistochemistry for Muc2 using the healing stage proximal colon specimens. PAS-positive cells and Muc2-positive cells were observed in the ulcerative region of Int-G_q/G_{11} DKO, but not in control (Figure 7*D*). Immunoreactivity of lysozyme was not observed and that of chromogranin A remained unchanged (data not shown). Nuclear staining of Hes1 was observed in the regenerating crypts of control mice, but it was greatly reduced in Int-G_q/G_{11} DKO colon (Figure 7*D*). Under physiological conditions, no differences in nuclear staining for Hes1 were observed between the 2 genotypes (Supplementary Figure 4). Next, we examined the proliferation of epithelial cells in the proximal colon using anti–Ki-67 antibody. In untreated mice, the rates of Ki-67–stained nuclei/total nuclei in control mice and Int-G_q/G_{11} DKO mice were 0.31 ± 0.03 and 0.30 ± 0.04, respectively ($P = .73$). In the acute colitis stage (day 5), the proliferation in the unaffected crypts was enhanced greatly in the control mice, whereas it was decreased severely in the Int-G_q/G_{11} DKO colon (control, 0.59 ± 0.02; Int-G_q/G_{11} DKO, 0.15 ± 0.05; $P < .01$). In the regenerating crypts of the Int-G_q/G_{11} DKO colon,

proliferation was decreased slightly on day 11 (control, 0.66 ± 0.06; Int-G_q/G_{11} DKO, 0.57 ± 0.11; $P = .30$), but it was decreased significantly on day 14 (control, 0.62 ± 0.01; Int-G_q/G_{11} DKO, 0.29 ± 0.06; $P < .01$). These results suggest that in DSS-induced colitis, proliferation was inhibited and the regenerative process was altered, with a tendency to differentiate toward goblet cells, not enterocytes, during the regeneration in Int-G_q/G_{11} DKO colon. Consequently, $G\alpha_{q/11}$ deficiency resulted in a poor survival rate during colitis.

Discussion

In this study, we used mice with a disruption of the *Gnaq* and *Gna11* gene to investigate the role of this trimeric G protein in regulating intestinal homeostasis. Signaling through $G\alpha_{q/11}$ is important in mediating the aspect of epithelial cell morphogenesis and plays a critical role in modulating the maturation of Paneth cells. It also plays a pivotal role in regeneration after DSS-induced colitis.

In light and electron microscopy, we noted a conspicuous population of cells in the Int-G_q/G_{11} DKO small intestine that was intermediate in appearance between Paneth and goblet cells (Figure 2). Such intermediate cells rarely are observed at crypt–villus junctions in wild-type small intestine and likely represent common progenitor cells of the Paneth and goblet cell lineages.[23,25] These cells have been reported to be observed during intestinal infection, inflammation, and the inhibition of Notch signaling.[29,34,35] Classic intermediate cells contain apical eosinophilic granules smaller than those in mature Paneth cells and contain both electron-lucent granules, as seen in goblet cells, and electron-dense granules, as seen in Paneth cells. In TEMs of Int-G_q/G_{11} DKO mice, we observed that Paneth cells gained features, suggestive of intermediate cells, with larger mucin-filled vacuoles than observed in classic intermediate cells. The number of intermediate cells was increased dramatically in Int-G_q/G_{11} DKO mice, and these cells were distributed ectopically along the crypt–villus axis (Figures 2 and 3). Similar but slight changes were observed in the G_{11} KO crypts but not in the Int-G_q KO crypts. This may be owing to the abundant expression of $G\alpha_{11}$ in comparison with $G\alpha_q$ in the mouse small intestine[5] (Figure 1*B*). Enterocytes remained unaltered in morphology and their polarity was not disturbed in Int-G_q/G_{11} DKO intestine. $G\alpha_{q/11}$ signaling might be dispensable in enterocytes or other $G\alpha_{q/11}$ family genes may be expressed and thus partially may compensate for the loss of $G\alpha_{q/11}$. However, signaling through $G\alpha_{q/11}$ appears to play a crucial role in the segregation of the Paneth/goblet cell lineages and in the terminal differentiation and maintenance of mature Paneth cell phenotype.

Paneth and goblet cells are thought to be closely related and emerge from a common progenitor cell.[36] As a consequence of losing the maturation of Paneth cells, we might observe an increase in goblet cell number in the crypts and villi of G_{11} KO and Int-G_q/G_{11} DKO mice (Figure 3). The control of intestinal stem cell fate, maintenance, and maturation depends on the correct dosing of Wnt/β-catenin signals along the crypt. Wnt/β-catenin signals promote a number of critical processes in the intestinal epithelium.[11] The key event in this signaling pathway is the stabilization of β-catenin and its interaction with Tcf transcription factors within the nucleus.[1] Interference with the Wnt pathway results in depletion of the Paneth cell lineage[26]; conversely, a loss of the key negative regulator of this pathway, Apc, results in an expansion of the Paneth cell lineage, indicating that proper development of the Paneth cell lineage requires fine tuning of β-catenin activation.[11,15,37] Because nuclear-localized β-catenin typically is observed only in Paneth cells, Paneth cell differentiation appears to require the highest levels of Wnt/β-catenin signal.[11,15] We found that nuclear β-catenin and Tcf1 was absent in Paneth cells of Int-G_q/G_{11} DKO crypt base, suggesting that signaling through $G\alpha_{q/11}$ modulates Wnt/β-catenin signaling in some way. The Wnt pathways include canonical Wnt signaling, which is referred to as Wnt/β-catenin pathway and noncanonical Wnt signaling, which is β-catenin–independent and subdivided into 2 general categories: the Wnt/Ca^{2+} and Wnt/c-Jun-N-terminal kinase pathways. Fzd is a 7-pass transmembrane receptor and is associated with heterotrimeric G protein in the Wnt/Ca^{2+} pathway, which activates phospholipase C-β and thereby the intracellular release of calcium. Induced calcium flux activates PKC and calcium-calmodulin–dependent kinase II, which can antagonize the Wnt/β-catenin pathway.[38] Mouse Fzd3, Fzd4, and Fzd6 activate PKC and calcium-calmodulin–dependent kinase II, but Fzd7 and Fzd8 do not affect their activity.[39] If this pathway plays a role, Wnt/β-catenin signaling is expected to be up-regulated under the condition of $G\alpha_{q/11}$-deficiency. Thus, in the mouse model of the present study, signaling through $G\alpha_{q/11}$ modulated Wnt/β-catenin signaling in another fashion.

Recent studies have suggested that Paneth cell lineage allocation and differentiation/maturation are regulated by distinct, but interacting, pathways. Specification of cells to the goblet and Paneth cell lineages involves numerous transcription factors, including Sox9, Atoh1, and SAM pointed domain-containing Ets transcription factor. Sox9, a high-mobility group box transcription factor expressed in intestinal crypt cells including Paneth cells, has been identified as a regulator of Paneth and goblet cell lineage specification in the intestine and colon.[14,27] Sox9, a direct transcriptional target of Wnt/β-catenin signaling, is needed for Paneth cell specification and Sox9-null mice lack Paneth cells in small intestine.[14,27] In fact, nuclear localization of Sox9 greatly was reduced in the crypt base of Int-G_q/G_{11} DKO intestine (Figure 5*C*). The sorting process of epithelial cells along the crypt–villus axis is dependent on the Wnt pathway via the modulation of ephrin-eph–receptor interactions.[1] EphB3 homozygous null mice show striking defects in the localization of Paneth cells, which are distributed randomly throughout the crypt.[1] However, in Int-G_q/G_{11} DKO mice, mRNA levels of EphB3 and EphB2 were not altered (Supplementary Figure 2). Rab8a knockout mice have been reported recently.[40] Wnt secretion is regulated partly by Rab8a-mediated anterograde transport. The deletion of Rab8a weakened the secretion of multiple Wnts, resulting in reduced Wnt signaling, defective Paneth cell maturation, and the expansion of leucine-rich

repeat-containing G-protein-coupled receptor 5–positive cells, which resembles the phenotype of Int-G_q/G_{11} DKO mice. However, intermediate cells, the mislocalization of Paneth cells, and an increased number of goblet cells are not reported in Rab8a KO mice, implying that other signals also are involved in the disturbance of Int-G_q/G_{11} DKO IECs.

Notch signaling in intestine also plays an important role as a gatekeeper of progenitor cells and a regulator to the absorptive/secretory lineage.[9] Inhibition of Notch signaling in the intestinal epithelium using conditional gene targeting of RBP-J or by pharmacologic γ-secretase inhibitors, which block the release of NICD, results in the loss of the proliferative crypt compartment and conversion of crypt progenitors into secretory cells.[9] The proliferative crypt cells express Notch1 and Notch2, whereas Dll1 and Dll4 function redundantly as Notch ligands.[28] Hes1 and Hes5 require Notch activation for transcription. Progenitor cells that express Hes1 will differentiate into absorptive enterocytes and those expressing Atoh1 are committed to the secretory lineage. Immunostaining of Dll1 and Hes1, Western blot of NICD1, and a qPCR of Dll1, Dll4, Notch1, Hes1, and Atoh1 did not show any alterations in the Int-G_q/G_{11} DKO IECs, other than an increase in the Hes5 mRNA level, suggesting that there was only a subtle alteration in the Notch signaling of the Int-G_q/G_{11} DKO IECs (Figure 5). The interaction of Notch signaling with the heterotrimeric G protein has not yet been reported.

Epithelial cells in small intestine communicate with the underlying mesenchymal components, including blood vessels, myofibroblasts, and immune cells, which secrete paracrine signals and collectively form the lamina propria.[41] Numerous trophic factors, including Wnts, fibroblast growth factors (FGFs), serotonin, and Indian hedgehog (Ihh) are known to influence the number of Paneth cells residing at the base of intestinal crypts.[15,42,43] In adult small intestine, mature Paneth cells may play a role in specification by steering progenitor cells away from the Paneth cell lineage through Ihh signaling, thereby controlling Paneth cell number.[44] Conversely, conditional knockout of Ihh in mouse small intestine results in an increased number of Paneth cells.[45,46] Recent evidence also suggests that signaling through FGF receptor 3 (Fgfr3) plays a critical role in Paneth cell maturation.[43] However, mRNA levels of Wnt5a, Ihh, and Fgfr3 remained unchanged in Int-G_q/G_{11} DKO intestine (Supplementary Figure 2).

Signaling through Wnt/β-catenin and the Tcf family transcription factors also plays a central role in proliferation during intestinal development.[13] We performed an in vivo BrdU incorporation assay to monitor proliferating cells among IECs. The total number of BrdU-positive cells did not differ between the 4 genotypes, however, when we focused on the crypt base (lower third of the crypt), the number of BrdU-positive cells was increased in G_{11} KO and Int-G_q/G_{11} DKO crypts (Figure 6*A*–*C*). A subsequent TUNEL assay showed that there were more apoptotic cells in only Int-G_q/G_{11} DKO crypts (Figure 6*D* and *E*) and unhealthy-looking cells occasionally were observed in TEM of Int-G_q/G_{11} DKO crypts (Figure 2*C*). These results suggest that proliferation at the crypt base might be activated to compensate for the loss of mature Paneth cells and apoptosis was induced only when the $G\alpha_q$ and $G\alpha_{11}$ both were deficient.

The colonic epithelium lacks Paneth cells and the morphologic architecture was preserved in Int-G_qKO, G_{11} KO, and Int-G_q/G_{11} DKO mice (Supplementary Figure 1*C*). We induced DSS colitis in control and Int-G_q/G_{11} DKO mice and examined the role of $G\alpha_{q/11}$ signaling in colon (Figure 7). $G\alpha_{q/11}$ deficiency significantly exacerbated the clinical course of DSS-induced colitis. Severe colitis was observed at day 5 and mucosal regeneration was disturbed in the regenerating stage compared with control mice. Cystic crypts were observed in the ulcerative area of the Int-G_q/G_{11} DKO colon, where PAS-positive and Muc2-positive cells were detected. Most of the cells in cystic crypts were Ki-67 negative (data not shown). Nuclear Hes1 immunoreactivity was decreased in the regenerating crypts of the Int-G_q/G_{11} DKO colon. The rate of Ki-67–positive cells showed that proliferation was reduced severely in the unaffected area during the acute colitis stage and in the regenerating area. It previously was reported that inhibition of Notch activation using a γ-secretase inhibitor resulted in a severe exacerbation of colitis, and activation of Notch promoted proliferation and regeneration by suppressing goblet cell differentiation.[47] As for Wnt signaling, no significant differences were observed in the regenerating crypts for the immunostaining of β-catenin, Tcf1, and Sox9. The band intensity of Tcf1 in Western blotting was reduced in the Int-G_q/G_{11} DKO colon, but this phenomenon may have been owing to the decreased regeneration of crypts in the Int-G_q/G_{11} DKO mice (Supplementary Figure 4). These results suggest that $G\alpha_{q/11}$ deficiency inhibited Notch signaling, decreased proliferation, and induced differentiation toward goblet cells in injured and regenerating areas, resulting in a higher mortality rate.

Taken together, the $G\alpha_{q/11}$-mediated signaling pathway plays a pivotal role in the maintenance of intestinal homeostasis, especially in Paneth cell maturation and positioning. $G\alpha_{q/11}$ deficiency has a significant effect on Wnt/β-catenin signaling and a slight effect on Notch signaling, which results in the altered differentiation of IECs. $G\alpha_{q/11}$ signaling also is indispensable for the regeneration of injured colonic epithelium. These new insights into signaling through $G\alpha_{q/11}$ may broaden our understanding of intestinal homeostasis and may lead us to a new therapeutic approach for enterocolitis, including inflammatory bowel disease.

References

1. Batlle E, Henderson JT, Beghtel H, et al. β-catenin and TCF mediate cell positioning in the intestinal epithelium by controlling the expression of EphB/EphrinB. Cell 2002;111:251–263.
2. Barker N, Clevers H. Tracking down the stem cells of the intestine: strategies to identify adult stem cells. Gastroenterology 2007;133:1755–1760.
3. Wank SA. I. CCK receptors: an exemplary family. Am J Physiol Gastrointest Liver Physiol 1998;274:G607–G613.
4. Robertson RP, Seaquist ER, Walseth TF. G proteins and modulation of insulin secretion. Diabetes 1991;40:1–6.

5. Strathmann M, Simon MI. G protein diversity: a distinct class of alpha subunits is present in vertebrates and invertebrates. Proc Natl Acad Sci U S A 1990; 87:9113–9117.
6. Exton JH. Regulation of phosphoinositide phospholipases by hormones, neurotransmitters, and other agonists linked to G proteins. Annu Rev Pharmacol Toxicol 1996;36:481–509.
7. Amatruda TT, Steele DA, Slepak VZ, et al. G alpha 16, a G protein alpha subunit specifically expressed in hematopoietic cells. Proc Natl Acad Sci U S A 1991; 88:5587–5591.
8. Wilkie TM, Scherle PA, Strathmann MP, et al. Characterization of G-protein alpha subunits in the Gq class: expression in murine tissues and in stromal and hematopoietic cell lines. Proc Natl Acad Sci U S A 1991; 88:10049–10053.
9. van Es JH, van Gijn ME, Riccio O, et al. Notch/[gamma]-secretase inhibition turns proliferative cells in intestinal crypts and adenomas into goblet cells. Nature 2005; 435:959–963.
10. van der Flier LG, Clevers H. Stem cells, self-renewal, and differentiation in the intestinal epithelium. Annu Rev Physiol 2009;71:241–260.
11. Andreu P, Peignon G, Slomianny C, et al. A genetic study of the role of the Wnt/β-catenin signalling in Paneth cell differentiation. Dev Biol 2008;324:288–296.
12. Fevr T, Robine S, Louvard D, et al. Wnt/β-catenin is essential for intestinal homeostasis and maintenance of intestinal stem cells. Mol Cell Biol 2007;27:7551–7559.
13. Korinek V, Barker N, Moerer P, et al. Depletion of epithelial stem-cell compartments in the small intestine of mice lacking Tcf-4. Nat Genet 1998;19:379–383.
14. Mori–Akiyama Y, van den Born M, van Es JH, et al. SOX9 Is required for the differentiation of Paneth cells in the intestinal epithelium. Gastroenterology 2007;133:539–546.
15. van Es JH, Jay P, Gregorieff A, et al. Wnt signalling induces maturation of Paneth cells in intestinal crypts. Nat Cell Biol 2005;7:381–386.
16. Zecchini V, Domaschenz R, Winton D, et al. Notch signaling regulates the differentiation of post-mitotic intestinal epithelial cells. Genes Dev 2005;19:1686–1691.
17. Yang Q, Bermingham NA, Finegold MJ, et al. Requirement of Math1 for secretory cell lineage commitment in the mouse intestine. Science 2001;294:2155–2158.
18. El Marjou F, Janssen K-P, Hung-Junn Chang B, et al. Tissue-specific and inducible Cre-mediated recombination in the gut epithelium. Genesis 2004;39:186–193.
19. Mashima H, Sato T, Horie Y, et al. Interferon regulatory factor-2 regulates exocytosis mechanisms mediated by SNAREs in pancreatic acinar cells. Gastroenterology 2011;141:1102–1113.e8.
20. Okayasu I, Hatakeyama S, Yamada M, et al. A novel method in the induction of reliable experimental acute and chronic ulcerative colitis in mice. Gastroenterology 1990;98:694–702.
21. Wettschureck N, Rutten H, Zywietz A, et al. Absence of pressure overload induced myocardial hypertrophy after conditional inactivation of G[alpha]q/G[alpha]11 in cardiomyocytes. Nat Med 2001;7:1236–1240.
22. Offermanns S, Zhao L-P, Gohla A, et al. Embryonic cardiomyocyte hypoplasia and craniofacial defects in Gαq. Gα11-mutant mice. EMBO J 1998;17:4304–4312.
23. Troughton WD, Trier JS. Paneth and goblet cell renewal in mouse duodenal crypts. J Cell Biol 1969;41:251–268.
24. Calvert R, Bordeleau G, Grondin G, et al. On the presence of intermediate cells in the small intestine. Anat Rec 1988;220:291–295.
25. Kamal M, Wakelin D, Ouellette AJ, et al. Mucosal T cells regulate Paneth and intermediate cell numbers in the small intestine of T. spiralis-infected mice. Clin Exp Immunol 2001;126:117–125.
26. Pinto D, Gregorieff A, Begthel H, et al. Canonical Wnt signals are essential for homeostasis of the intestinal epithelium. Genes Dev 2003;17:1709–1713.
27. Bastide P, Darido C, Pannequin J, et al. Sox9 regulates cell proliferation and is required for Paneth cell differentiation in the intestinal epithelium. J Cell Biol 2007;178:635–648.
28. Pellegrinet L, Rodilla V, Liu Z, et al. Dll1- and Dll4-mediated notch signaling are required for homeostasis of intestinal stem cells. Gastroenterology 2011;140:1230–1240.e7.
29. VanDussen KL, Carulli AJ, Keeley TM, et al. Notch signaling modulates proliferation and differentiation of intestinal crypt base columnar stem cells. Development 2012;139:488–497.
30. Schröder N, Gossler A. Expression of Notch pathway components in fetal and adult mouse small intestine. Gene Expr Patterns 2002;2:247–250.
31. Bjerknes M, Cheng H. Cell Lineage metastability in Gfi1-deficient mouse intestinal epithelium. Dev Biol 2010; 345:49–63.
32. Gregorieff A, Stange DE, Kujala P, et al. The Ets-domain transcription factor Spdef Promotes maturation of goblet and Paneth cells in the intestinal epithelium. Gastroenterology 2009;137:1333–1345.e3.
33. Shorning BY, Zabkiewicz J, McCarthy A, et al. Lkb1 deficiency alters goblet and Paneth cell differentiation in the small intestine. PLoS One 2009;4:e4264.
34. Vidrich A, Buzan JM, Barnes S, et al. Altered epithelial cell lineage allocation and global expansion of the crypt epithelial stem cell population are associated with ileitis in SAMP1/YitFc mice. Am J Pathol 2005;166:1055–1067.
35. Walsh R, Seth R, Behnke J, et al. Epithelial stem cell-related alterations in Trichinella spiralis-infected small intestine. Cell Prolif 2009;42:394–403.
36. Crosnier C, Stamataki D, Lewis J. Organizing cell renewal in the intestine: stem cells, signals and combinatorial control. Nat Rev Genet 2006;7:349–359.
37. Sansom OJ, Reed KR, Hayes AJ, et al. Loss of Apc in vivo immediately perturbs Wnt signaling, differentiation, and migration. Genes Dev 2004;18:1385–1390.
38. Lien W-H, Fuchs E. Wnt some lose some: transcriptional governance of stem cells by Wnt/β-catenin signaling. Genes Dev 2014;28:1517–1532.
39. Kohn AD, Moon RT. Wnt and calcium signaling: β-catenin-independent pathways. Cell Calcium 2005; 38:439–446.
40. Das S, Yu S, Sakamori R, et al. Rab8a vesicles regulate Wnt ligand delivery and Paneth cell maturation at the intestinal stem cell niche. Development 2015;142:2147–2162.

41. Powell DW, Pinchuk IV, Saada JI, et al. Mesenchymal cells of the intestinal lamina propria. Annu Rev Physiol 2011;73:213–237.
42. Brodrick B, Vidrich A, Porter E, et al. Fibroblast growth factor receptor-3 (FGFR-3) regulates expression of paneth cell lineage-specific genes in intestinal epithelial cells through both TCF4/β-catenin-dependent and -independent signaling pathways. J Biol Chem 2011;286:18515–18525.
43. Vidrich A, Buzan JM, Brodrick B, et al. Fibroblast growth factor receptor-3 regulates Paneth cell lineage allocation and accrual of epithelial stem cells during murine intestinal development. Am J Physiol Gastrointest Liver Physiol 2009;297:G168–G178.
44. Varnat F, Heggeler BBT, Grisel P, et al. PPARβ/δ regulates paneth cell differentiation via controlling the hedgehog signaling pathway. Gastroenterology 2006;131:538–553.
45. Kosinski C, Stange DE, Xu C, et al. Indian hedgehog regulates intestinal stem cell fate through epithelial–mesenchymal interactions during development. Gastroenterology 2010;139:893–903.
46. van Dop WA, Heijmans J, Büller NVJA, et al. Loss of Indian hedgehog activates multiple aspects of a wound healing response in the mouse intestine. Gastroenterology 2010;139:1665–1676.e10.
47. Okamoto R, Tsuchiya K, Nemoto Y, et al. Requirement of Notch activation during regeneration of the intestinal epithelia. Am J Physiol Gastrointest Liver Physiol 2009; 296:G23–G35.

Received December 17, 2015. Accepted August 15, 2016.

Correspondence
Address correspondence to: Hirosato Mashima, MD, PhD, Department of Gastroenterology, Saitama Medical Center, Jichi Medical University, Saitama 330-8503, Japan. e-mail: hmashima1-tky@umin.ac.jp; fax: (81) 48-648-5188.

Acknowledgment
The authors thank Chihiro Taira, Hitoshi Watanabe, Sachiko Fujita, Keiko Iwamoto, and Shinsuke Chida for their excellent technical assistance.

Conflicts of interest
The authors disclose no conflicts.

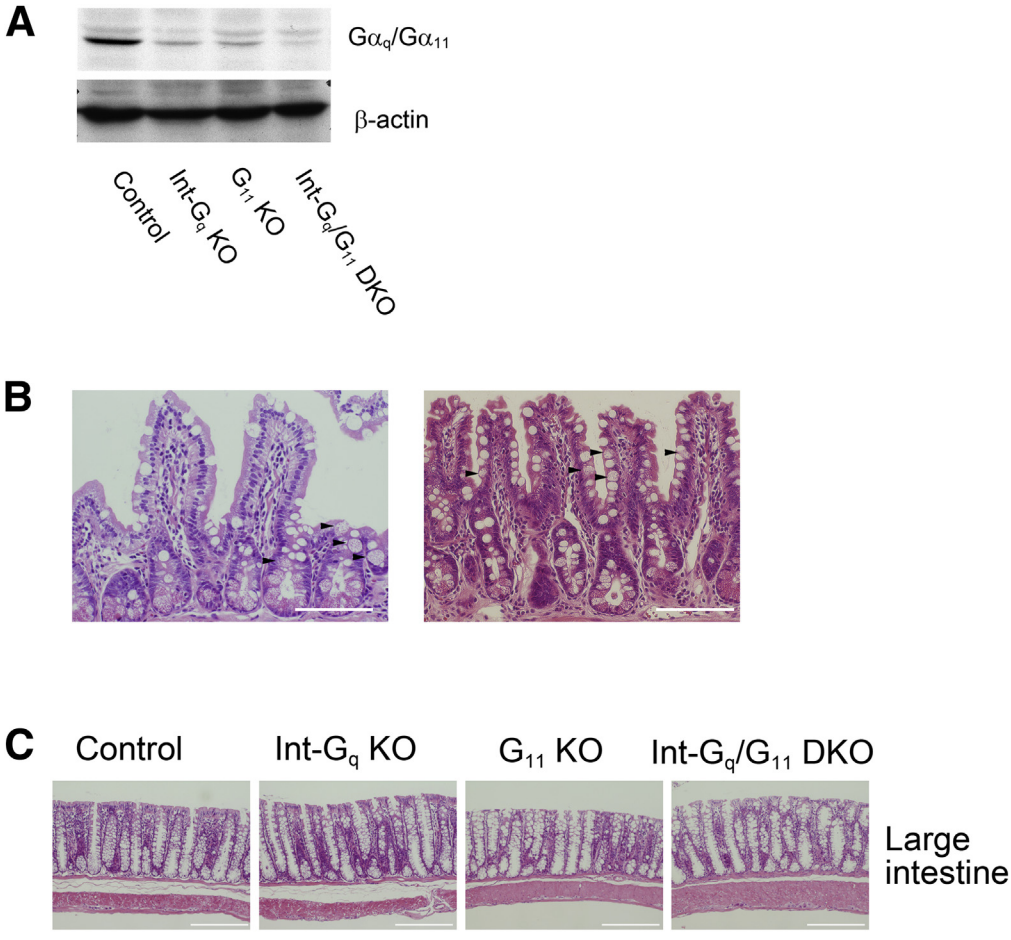

Supplementary Figure 1. (*A*) Western blot analysis of $G\alpha_q/G\alpha_{11}$ expression in 4 mouse lines: control (*Gnaq*$^{flox/flox}$*Gna11*$^{+/+}$), Int-G_q KO (*VilCre*$^{+/-}$*Gnaq*$^{flox/flox}$ *Gna11*$^{+/+}$), G_{11} KO (*Gnaq*$^{flox/flox}$*Gna11*$^{-/-}$), and Int-G_q/G_{11} DKO (*VilCre*$^{+/-}$*Gnaq*$^{flox/flox}$*Gna11*$^{-/-}$). (*B*) H&E staining in small intestine of Int-G_q/G_{11} DKO mice. Enlarged Paneth cells were distributed along the crypt–villus axis. (*C*) HE staining in large intestine of 4 mouse lines. Morphologic changes were not detected. *Scale bars*: 200 μm.

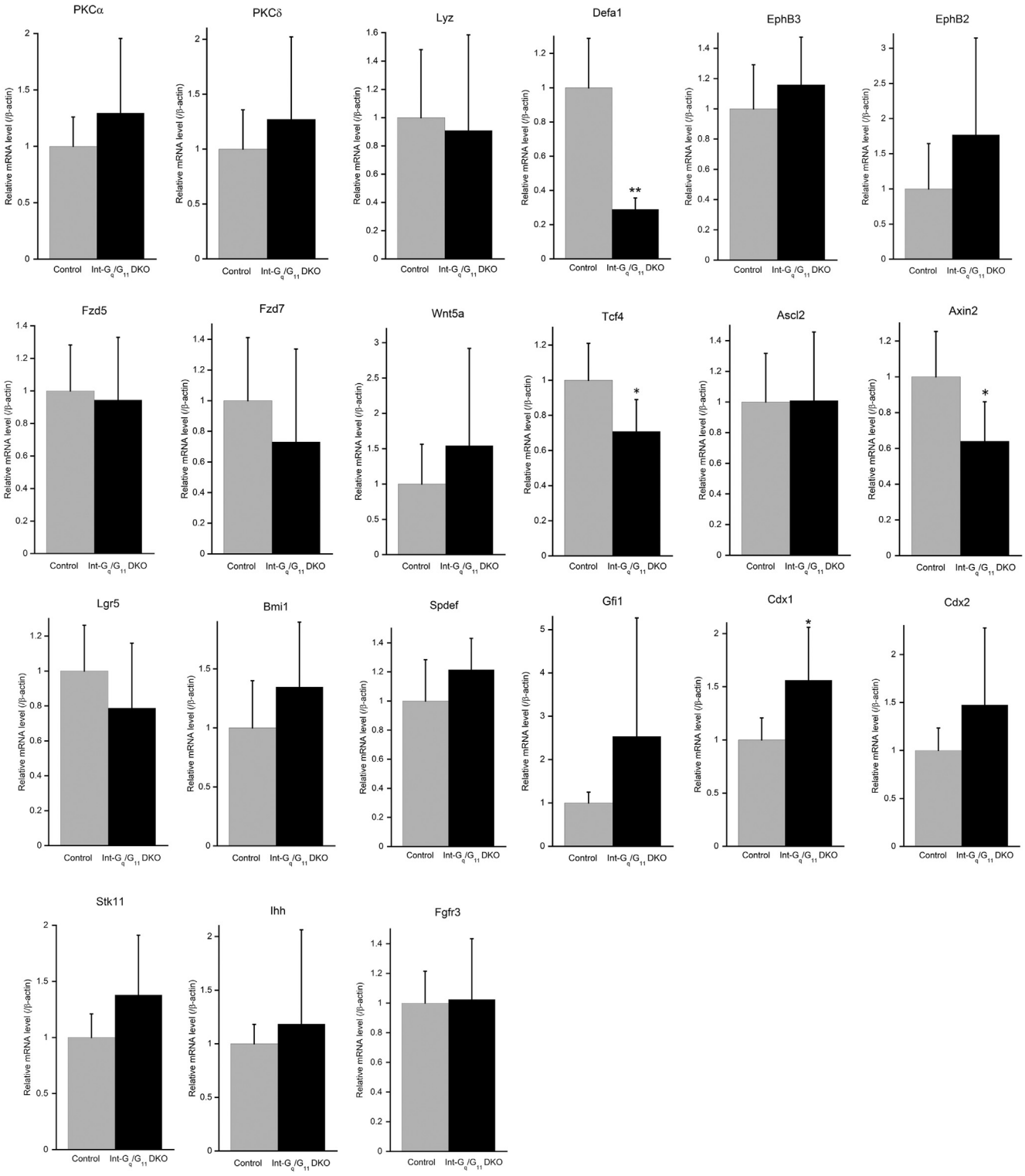

Supplementary Figure 2. Relative expression of Paneth cell markers (Lyz, Defa1), stem cell markers (leucine-rich repeat-containing G-protein-coupled receptor 5 [Lgr5], Bmi1), transcription factors (Cdx1, Cdx2, spdef), Wnt/β-catenin signaling molecules (Fzd5, Fzd7, Wnt5a), Notch signaling molecules (Dll4, Notch1, Hes1, Atoh1), receptors (EphB3, EphB2, Fgfr3), and others (Stk11 [LKB1], Ihh) were measured by quantitative real-time PCR. Data represent the means ± SD of 3 mice per genotype from 2 independent experiments. *$P < .05$, **$P < .01$, according to analysis of variance.

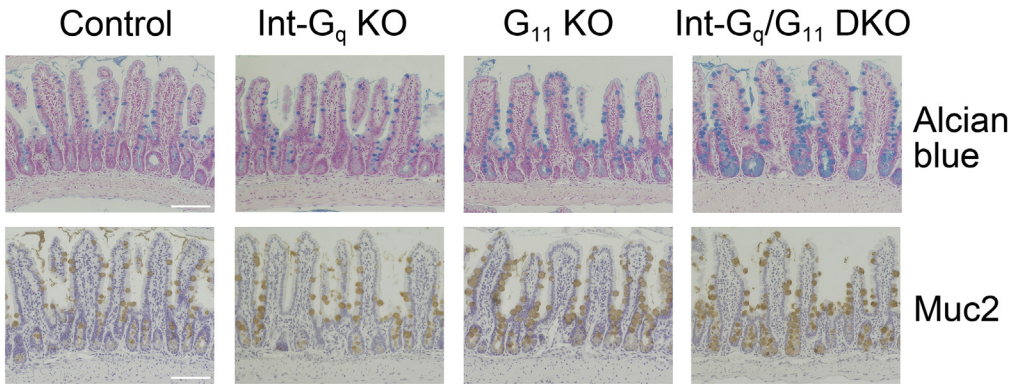

Supplementary Figure 3. Alcian blue staining and immunohistochemistry of Muc2 in Int-G_q/G_{11} DKO small intestine. *Scale bars*: 100 μm.

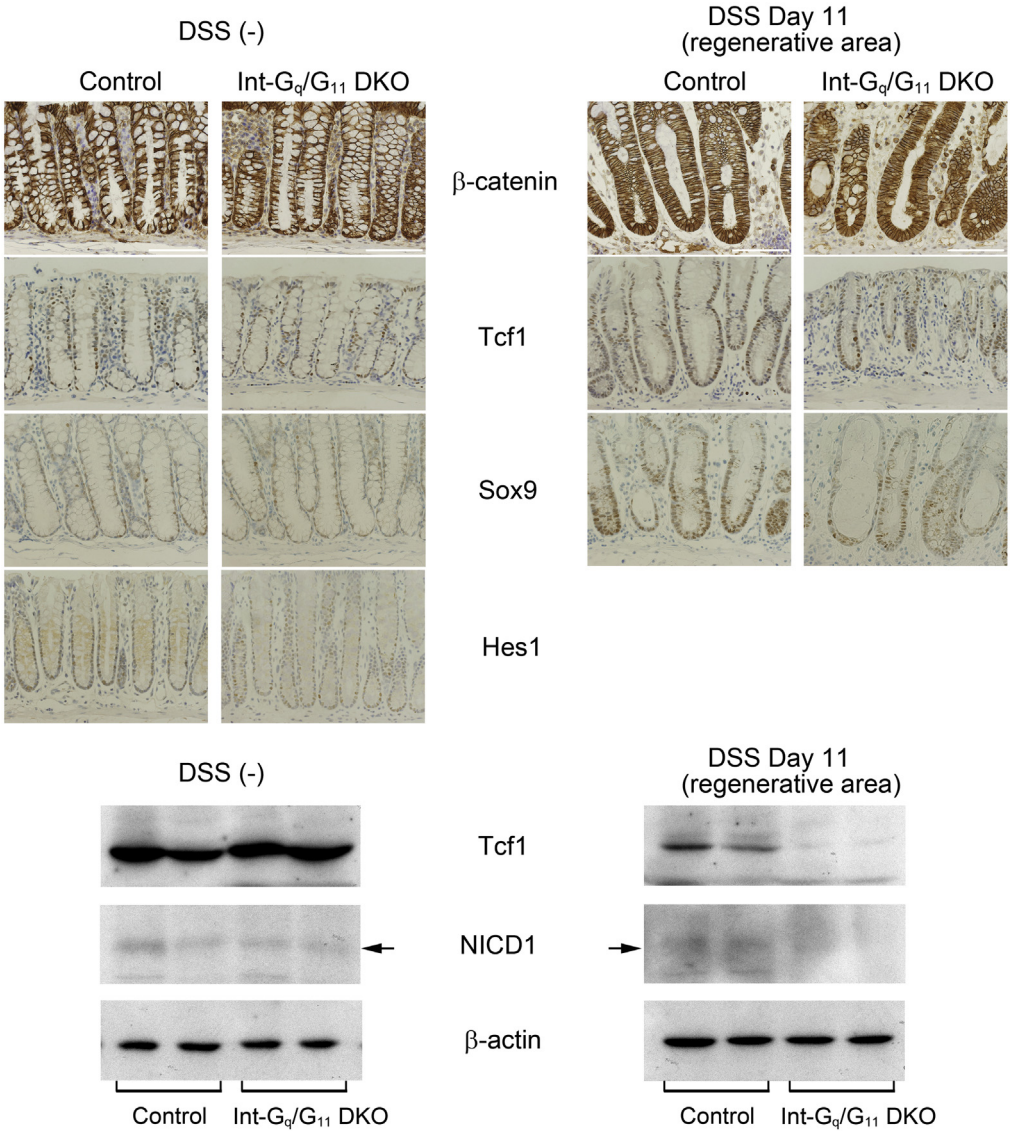

Supplementary Figure 4. Immunohistochemical studies were performed for β-catenin, Tcf1, Sox9, and Hes1 in control and Int-G_q/G_{11} DKO mice using DSS-untreated and DSS-treated colonic specimens. *Scale bars*: 100 μm. Western blot was performed for the Tcf1, NICD1, and β-actin using proximal colonic mucosa, which was scraped off of colon tissue with a spatula (n = 2).

Supplementary Table 1. The Primers Used in the Present study

Gene name	Accession no		Primer sequence	Size	Annealing temperature	
Genotyping						
$Gna11^{+}$		F	GCCCCTTGTACAGATGGCAG	820 bp	60°C	
		R	AGCATGCTGTAAGACCGTAG			
$Gna11^{-}$		F	CAGGGGTAGGTGATGATTGTGC	450 bp	60°C	
		R	GACTAGTGAGACGTGCTACTTCC			
$Gnaq^{+}$		F	AGCTTAGTCTGGTGACAGAAGC	600 bp	60°C	
$Gnaq^{flox}$		R	GCATGCGTGTCCTTTATGTGAG	700 bp		
Cre recombinase		F	CAATTTACTGACCGTACAC	1026 bp	60°C	
		R	TAATGCCATCTTCCAGCAG			
Reverse-transcription PCR						
Gnaq	NM_008139	F	TGGACCGTGTAGCCGACCCT	270 bp	60°C	
		R	GTGCTTTGCTCTCCTCCATGCGG			
Gna11	NM_010301	F	ACGAGGTGAAGGAGTCGAAGC	573 bp	60°C	
		R	CCATCCTGAAGATGATGTTCTCC			
Actb	NM_007393	F	TGAGAGGGAAATCGTGCGTG	460 bp	60°C	
		R	GATCCACATCTGCTGGAAGGTG			
Real-time PCR						
1 PKCα	NM_011101	F	GCTTCCAGTGCCAAGTTTGC	76 bp	60°C	
		R	GCACCCGGACAAGAGAACGTAA			
2 PKCδ	NM_011103	F	TATCAACTGGTCCCTCCTGG	105 bp	60°C	
		R	CATTCAGGAACTCTGGGTCA			
3 Lyz	NM_013590	F	GGTCTACAATCGTTGTGAGTTGG	387 bp	65°C	
		R	CTCCGCAGTTCCGAATATACT			
4 Defa1	NM_010031	F	TCAAGAGGCTGCAAAGGAAGAGAAC	94 bp	60°C	
		R	TGGTCTCCATGTTCAGCGACAGC			
5 EphB3	NM_010143	F	CCATAGCCTATCGGAAGTTTACGT	87 bp	60°C	
		R	TCGCTCTCCGTAGCTCATGAC			
6 EphB2	NM_001290753	F	CTCTACTGTAACGGGGACGG	119 bp	60°C	
		R	TTGAAGGTTCCTGATGGACA			
7 Fzd5	NM_001042659	F	GTGCTTCATCTCCACGTCCA	103 bp	60°C	
		R	CAGGTAGCACGCAGACAAGA			
8 Fzd7	NM_008057	F	ACCCTACTGCTCCCTACCTG	84 bp	60°C	
		R	AGAAGGGGAAAGACAAGCGG			
9 Wnt5a	NM_009524	F	ACAGGCATCAAGGAATGCCA	104 bp	60°C	+DMSO
		R	CGGCTGCCTATTTGCATCAC			
10 Tcf4	NM_013685	F	AGCCCGTCCAGGAACTATG	101 bp	60°C	
		R	TGGAATTGACAAAAGGTGGA			
11 Ascl2	NM_008554	F	TCCAGTTGGTTAGGGGGCTA	107 bp	60°C	
		R	GCATAGGCCCAGGTTTCTTG			
12 Axin2	NM_015732	F	TGAGATCCACGGAAACAGC	104 bp	60°C	
		R	GTGGCTGGTGCAAAGACAT			
13 Dll1	NM_007865	F	GGAGAAGATGTGCGACCCT	103 bp	60°C	
		R	CTCCCCTGGTTTGTCACAGT			
14 Dll4	NM_019454	F	ATGGGGAGGTCTGTTTTGTG	101 bp	60°C	
		R	TATAACCCTTTGGCCCACTG			
15 Notch1	NM_008714	F	CAAGAGGCTTGAGATGCTCC	132 bp	65°C	
		R	AAGGATTGGAGTCCTGGCAT			
16 Hes1	NM_008235	F	CTGGTGCTGATAACAGCGGA	80 bp	60°C	
		R	AGGGCTACTTAGTGATCGGT			
17 Hes5	NM_010419	F	CAAGGAGAAAAACCGACTGCG	188 bp	60°C	+DMSO
		R	CGAAGGCTTTGCTGTGTTTCA			
18 Atoh1	NM_007500	F	GTGCGATCTCCGAGTGAGAG	108 bp	60°C	
		R	GGGATAAGCCCCGAACAACA			
19 Lgr5	NM_010195	F	CAACCTCAGCGTCTTCACCT	96 bp	60°C	+DMSO
		R	TCTTCTAGGAAGCAGAGGCG			
20 Bmi1	NM_007552	F	CTTTCATTGTCTTTTCCGCC	90 bp	60°C	
		R	TGGTTGTTCGATGCATTTCT			
21 Spdef	NM_013891	F	CACGTTGGATGAGCACTCGCTA	142 bp	60°C	
		R	AGCCACTTCTGCACGTTACCAG			
22 Gfi1	NM_010278	F	GGCAAAAGATTCCACCAGAA	110 bp	60°C	
		R	TTGGAGCTCTGACTGAAGGC			
23 Cdx1	NM_009880	F	GACGCCCTACGAATGGATGC	80 bp	60°C	
		R	ACTTGTCCTTGGTTCGGGTC			
24 Cdx2	NM_007673	F	CCTACCCACGAACAGCATCTACT	69 bp	60°C	
		R	CCTGAGGTCCATAATTCCACTCA			

Supplementary Table 1. Continued

	Gene name	Accession no		Primer sequence	Size	Annealing temperature
25	Stk11 (Lkb1)	NM_001301853	F	CTACTCCGAGGGATGTTGGA	115 bp	60°C
			R	GATAGGTACGAGCGCCTCAG		
26	Ihh	NM_010544	F	GACTCATTGCCTCCCAGAACTG	150 bp	60°C
			R	CCAGGTAGTAGGGTCACATTGC		
27	Fgfr3	NM_001163215	F	TCGTGGCTGGAGCTACTTC	95 bp	60°C
			R	CTCCTGCTGGCTAGGTTCAG		
28	Actb	NM_007393	F	CTTCCTCCCTGGAGAAGAGC	101 bp	60°C
			R	AAGGAAGGCTGGAAAAGAGC		

DMSO, dimethyl sulfoxide; F, forward; Lgr5, leucine-rich repeat-containing G-protein-coupled receptor 5; R, reverse; Spdef, SAM pointed domain-containing Ets transcription factor.

Supplementary Table 2. The Primary Antibodies Used in the Present Study

	Company	Catalog no	Dilution
Alkaline phosphatase	Rockland, Limerick, PA	200-4135	1:2000
β-actin	Santa Cruz, Dallas, TX	sc-1616	1:1000
β-catenin	BD Biosciences, San Jose, CA	610154	1:50
BrdU	Sigma-Aldrich, St. Louis, MO	B2531	1:1000
Chromogranin A	Abcam, Cambridge, United Kingdom	ab15160	1:100
Dll1	R&D Systems, Minneapolis, MN	AF5026	1:500
E-cadherin	BD Biosciences, San Jose, CA	c20820-050	1:200
FITC-phalloidin	Sigma-Aldrich, St. Louis, MO	P5282	1:1000
Gnaq/Gna11	Abcam, Cambridge, United Kingdom	ab79337	1:200
Hes-1	Santa Cruz, Dallas, TX	sc-25392	1:150
Hes-5	Millipore, Darmstadt, Germany	AB5708	1:200
Ki-67	Cell Signaling, Danvers, MA	12202	1:800
Lysozyme	Dako, Glostrup, Denmark	A0099U2	1:1000
Muc2	Santa Cruz, Dallas, TX	sc-15334	1:200
Notch1	Abcam, Cambridge, United Kingdom	ab27526	1:200
Phospho-PKC (pan)	Cell Signaling, Danvers, MA	9371	1:1000
Sox9	Millipore, Darmstadt, Germany	AB5535	1:200
Tcf1	Cell Signaling, Danvers, MA	2203	1:100

FITC, fluorescein isothiocyanate.